published in Vol 33 of Studies of High Temperature Superconductors (A.Narlikar, ed.), pp 73. Nova Science Publishers (2000).

Ac loss in superconducting power cables

M.Däumling[1], S. Krüger Olsen[2], C.Træholt[2], D.W.A.Willén [1], A.Kühle[2,3], C.N.Rasmussen[1], C.Rasmussen[2], O.Tønnesen[2], J. Østergaard[4]
[1] NKT Research Center, Priorparken 878, DK-2605 Brøndby
[2] Danish Technical University, Dept. of Electric Power Engineering, Build. 325, DK-2800 Lyngby
[3] now at: Danish Institute of Fundamental Metrology, Anker Engelunds Vej 1, DK-2800 Lyngby, Denmark
[4]DEFU, Research Institute of Danish Electric Utilities, P.O.Box 259, DK-2800 Lyngby, Denmark

1. INTRODUCTION

Superconducting power cables have been of considerable interest since the discovery of the high T_c superconducting materials [1-7]. Most projects use conductors made of typically the $(Bi,Pb)_2Sr_2Ca_2Cu_3O_{10+x}$ (Bi2223) material. Attractive is the larger amount of current and energy that can be transferred using superconductors compared to copper cables and the energy savings that can be obtained with the superconductor. There is a loss associated with the transport of an ac in superconductors even though dc can be conducted virtually without loss. It is this loss onto which this chapter focuses. It should be noted that this chapter is rather a summary of our work than a review of the literature on the subject.
The basis of all applications of a superconductor in engineering is a composite conductor, containing the superconductor itself, and in the most simple case a metallic matrix. In more complicated conductors the matrix may consist of several metals, resistive barriers and mechanical reinforcements. Depending on the requirements for use single conductors may need to be bundled, either straight or twisted, or transposed for use in power cables. Due to the layered nature of the Bi2223 material it is usually fabricated in the form of a tape.

Three different kinds of losses occurring in the conductor must be distinguished. These are losses originating from a) eddy current losses in the matrix, b) hysteresis losses in the superconductor itself, and c) losses from coupling of the different strands or filaments of the composite conductor. Depending on the application normally c) poses the largest challenges to engineers. In a power cable additional losses in the cryostat and shield and losses due to the interaction of the conductors must be considered.
In this chapter first the losses from the tape conductor used to build up the superconducting cable are considered. Then the conductors are combined to a superconducting power cable, and loss mechanisms there are discussed. This chapter is not trying to review power cables in general, but give a description of the current generation of power cables (shown in figure 1) from our point of view, summarising previous work on the subject. These cables consist of several layers wound onto a central former that carries the coolant for the cable. The layers themselves are wound with tape conductors that contain the superconducting material, usually in the form of many filaments. The layers are electrically insulated from each other by a layer of for example Mylar tape, and soldered together at the ends of the cable. Three phase cables are not treated in this chapter.

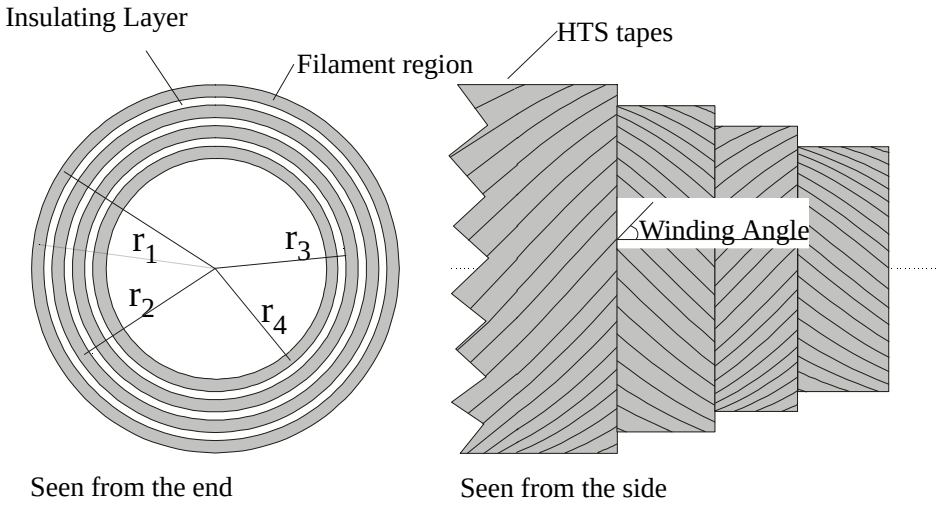

Figure 1. Schematic view of a four layer cable conductor.

2. AC LOSS IN SUPERCONDUCTING TAPES

2.1 Critical State Model and Hysteresis Losses

A superconductor is usually thought of a conductor without electric resistance. However, this is only true if the whole of the superconductor is not exposed to magnetic fields above its lower critical field H_{c1}, bearing in mind that demagnetisation effects will enhance the local magnetic field depending on the shape of the superconductor. Below H_{c1} the superconductor behaves as an ideal diamagnet with a susceptibility of -1 [8]. This statement is also valid in the sense of Silsbee's rule for applied transport current - which

states that as long as the self field of the transport current applied is below H_{c1} it will be carried without loss in a surface sheath of thickness λ, the magnetic penetration depth. In practice, this regime is usually meaningless, as the values of current to be carried and fields encountered usually exceed H_{c1} manifold. This is in particular true for the anisotropic high temperature superconductors that have very low values of H_{c1}.
A typical value of H_{c1} for YBCO at 77K is around 5000A/m, H || c. For Bi2223 H_{c1} is not exactly known, but is significantly smaller than for YBCO [9].

If the applied magnetic field H exceeds H_{c1}, which is usually the case, an ac can no longer be carried without loss. The magnetic field has penetrated the superconductor in the form of quantified magnetic flux lines. If a transport current (ac or dc) is applied in this case, losses occur due to the movement of the magnetic flux lines causing dissipation. In case the fluxons cannot move freely in the specimen, it has a finite critical current density j_c. For electrical engineering purposes the microscopic origins of j_c are usually ignored, and so we shall be content that the superconductor has a well-defined critical current density j_c, at which it develops a certain voltage, for example 1 μV/cm. In case of a sharp transition, below j_c its dc resistivity is 0, and above j_c its dc resistivity is its flux flow resistivity (more gradual transitions: see section 3.2). In order to avoid other complications for practical purposes we also assume that the reversible magnetisation $M_{rev}=0$ and $H_{c1}=0$, which is implied for the rest of this work, unless otherwise mentioned. This leads to the hysteretic response of the superconductor to an applied magnetic field that is usually described as the critical state or Bean state [10].
In the slab geometry (slab of width 2a extending infinitely along y and z directions) the slope of the local magnetic field is given by the Maxwell equation *curl* $\mathbf{H} = \mathbf{j} = \mathbf{j_c}$. Thus an applied field H parallel to the z direction leads to $dH/dx = j_c$. Corresponding to the penetration of the magnetic field a current density $j=|j_c|$ flows where the magnetic field has penetrated (positive on one side, negative on the other). Is the direction of the field ramp reversed, then the current of opposite polarity penetrates from the specimen borders. A characteristic field $H^* = j_c a$ (full penetration field) can be defined, which is the magnetic field at which the flux front penetrates to the centre of the slab [11].
One notes that the currents behave anti-symmetric, and the fields symmetric with respect to the middle of the specimen. A slab carrying a transport current reverses the role of current and field: all of the current is going the same direction, producing anti-symmetric field distributions. Like the magnetic fields, currents penetrate from the outside to inside.

2.2 Slab in parallel magnetic field

Let the applied field be $H=H_0 \sin(\omega t)$. Then the flux in the specimen can be reconstructed from the critical state model. Typically the energy loss per unit volume per cycle ($\omega=1$ for convenience) is schematically obtained from

(1) $$P = \frac{1}{\delta}\int_{-\delta/2}^{\delta/2} \frac{d\ddot{o}}{dt}\, j dt$$

Hereby making use of the partial integration rule leads to

(2) $$P = \frac{1}{p}(f(p/2) - f(-p/2)) - \frac{1}{p}\int_{-p/2}^{p/2} f\,\frac{dj}{dt}\,dt$$

In the quasistatic approach the second term is neglected (dj/dt=0). This leads to a power loss per volume of (now f = frequency = $\omega/2\pi$)

(3) $$\frac{P}{V} = \frac{2\hat{\imath}_0 f H_0^3}{3 j_c a}$$

where 2a is the width of the slab, valid for $H_0 < H^* = j_c a$. The loss increases with the cube of the applied magnetic field. If $H_0 > H^*$ the loss/volume is composed of two terms, that of equation 3 for $H_0 = H^*$, and

(4) $$P/V = f \mu_0 j_c a (H_0 - H^*)$$

This loss corresponds to the saturation of the shielding in the specimen and only depends linearly on field. It also depends linearly on the size of the slab, which is one of the reasons for finely subdividing superconductors that are used in changing external magnetic fields (more see [12]).

2.3 Slab carrying transport current in a magnetic field

In this case the slab is carrying a current $I = I_i \sin(\omega t)$, and is exposed to an in phase parallel magnetic field $B = B_{tot} \sin(\omega t) = \mu_0 H_{tot} \sin(\omega t)$. This has been treated [13] using the critical state model. Recently measurements in Bi2223 tapes have shown that these expressions give a good estimate of the ac loss [14] for fully coupled, non-twisted, multifilamentary tapes. The loss P per cycle per volume V is given by (f is the frequency = $\omega/(2\pi)$)

(5) $$\frac{P}{Vf} = \frac{2B_p}{3\hat{\imath}_0}(i^3 + 3\hat{a}^2 i) \qquad \text{for } \beta < i$$

(6) $$\frac{P}{Vf} = \frac{2B_p}{3\hat{\imath}_0}(\hat{a}^3 + 3\hat{a}\, i^2) \qquad \text{for } i < \beta < 1$$

(7) $$\frac{P}{Vf} = \frac{2B_p}{3\mu_0}\left(\hat{a}(3+i^2) - 2(1-i^2) + 6i^2\frac{(1-i)^2}{(\hat{a}-i)} - 4i^2\frac{(1-i)^3}{(\hat{a}-i)^2}\right) \qquad \text{for } \beta>1$$

Hereby P is the total power loss and $i=I_i/I_{ci}$, $\beta=H_{tot}/H^*$, and $B_p=\mu_0 H^*$.

2.4 Strip in perpendicular field

In a single-phase cable conductor without a gap between tapes (as shown in figure 1) all of the magnetic fields are oriented parallel to the conducting tape. However, in case of imperfect orientation or when there is a gap between tapes or in the presence of other current carrying conductors magnetic fields may be present that are oriented perpendicular to the surface of the tape. The power loss can be determined using a similar integration technique to the one described above [15]. However, the flux profiles are different and non-linear due to the demagnetisation field occurring at the strip edges. The power loss/length is given by [15]

(8) $P/l = 4\,\mu_0\, f\, j_c\, t\, a^2\, H_0\; h(H_0/H_c)$ for $H_0 < H_c$

(9) $P/l = 4\,\pi\,\mu_0\, f\, a^2\, j_c\, t\;\; (H_0 - 1.386\, H_c)$ for $H_0 >> H_c$

The strip has the width 2a, and thickness t, and $H_c=j_c\, t\,/\pi$, and the function $h(x) = (2/x)\ln(\cosh x) - \tanh x$. For $H_0<<H_c$ the loss is proportional to H_0^4.

2.5 Strip or ellipse carrying a transport current

Now the strip is carrying a transport current $I=I_0 \sin(\omega t)$. If I_c is the critical current of the strip, the power loss/length is

(10) $P/l = f\,\mu_0\, I_c^2\, g(I_0/I_c)\,/\,\pi$

Where $g(x) = (1-x)\ln(1-x) + (1+x)\ln(1+x) - x^2$. This is usually referred to as the Norris strip formula [16]. For low currents $I_0<<I_c$ it behaves as

(11) $P/l = f\,\mu_0\, I_0^4\,/\,(6\pi\, I_c^2)$

The ac loss behaviour of a strip of not rectangular but elliptical cross-section is significantly different. In particular at low I_0/I_c values the strip has significantly lower losses. The Norris ellipse formula [16] gives the power loss as

(12) $P/l = f\,\mu_0\, I_c^2\, e(I_0/I_c)\,/\,(2\pi)$

Where the function e(x) = (2-x) x + 2 (1-x) ln(1-x). This expression is valid for ellipses of all aspect ratios, thus also for a round wire. However, it turns out that losses for a strip of finite thickness tend to be significantly higher than that of the Norris strip (determined numerically [17]).

2.6 Tube carrying transport current (monoblock model)

Now we look at the case of a solid tube carrying a transport current. This case is relevant for a cable since (unless special measures are taken) typically the outer layers fill up with current first, corresponding to a solid tube. When a current is applied it penetrates homogeneously from the outer radius R to the inside radius r. The magnetic field created is oriented tangentially to the surface, and perpendicular to the current. If (R-r)<<R then the field profile created by the current is linear and resembles half of the critical state model for a slab. As the current is increased from 0 to I_c a flux front penetrates from R to r. The magnetic field at and inside of the flux front is 0, and the slope $dH/d\rho = j_c$ (where ρ denotes the radial co-ordinate). The calculation of the loss takes place in a similar fashion to the slab case by integrating the flux at its maximum value (see above).
The resulting loss/length is [18]

(13) $$P/l = \frac{\mu_0}{2\pi}\frac{I_c^2}{h^2} f[(2-h)h + 2(1-h)\ln(1-h)]$$

where $\beta=I_0/I_c$, and $h=1-(r/R)^2$.
For a solid rod (h=1) the result is identical to the Norris elliptical formula given above. The function in the square brackets is for most of the range of β proportional to β^3. Thus for a given current I_0 the power loss $P \propto I_0^3/I_c$. In connection with a power cable this solid tube model is usually referred to as the monoblock model [18].

2.7 Measurement of ac loss in tapes

The ac loss of a transport current can most easily be measured in a 4-probe configuration. Thereby the voltage drop over the specimen is measured directly with voltage contacts, the leads of which are lead straight away perpendicularly several tape widths from the tape before being twisted [19].
The current and its phase can be measured using either a Rogowski coil or a non-inductive shunt resistance. The voltage can either be measured phase sensitively with a Lock-In amplifier (more detail see section 3.6.2), or the whole waveform of the voltage is recorded on a digital oscilloscope, where it can be folded with the current directly to give the power loss [20]. Commercial power meters are usually useless as the voltages that need to be measured are in the nV to μV regime, thus very small.
It must be noted that – unless compensation is used – the demands on the sensitivity and accuracy of the Lock-In amplifier are enormous. Even a small phase error can easily

produce erroneous results [21]. A phase measurement to better than 0.01 degrees is needed in order to measure the ac loss at I/I_c=0.1 with an error of about +/- 20%. To add compensation, however, generally adds complexity to the system, and thus additional sources of error, so that many laboratories work in fact without compensation.
Losses incurred by a magnetic field are usually measured by measuring the magnetic moment m of the specimen as a function of applied magnetic field H. The power loss per cycle is then given by the area of the enclosed loop $P = \oint mdH$.

The magnetic moment can be measured either by using commercial magnetometers, by ac susceptometry, or indirectly with Hall probes that measure the magnetic field above the specimen. At power frequencies typically ac susceptometry is used.
The combined effect of transport currents and magnetic fields can be measured with a rather elaborate version of a standard set-up, using non-inductively placed voltage tabs.
Non-electrical methods of loss measurements usually involve measuring the heat generated by the power loss. This can be done by measuring the temperature rise of an adiabaticly placed specimen [22,23], or by measuring the boiloff of the coolant used (liquid nitrogen or helium)[24]. An alternative method is the resonance method (see below), which however has never been used with single tapes.

3. POWER CABLES

3.1 Self and mutual inductances

The geometry of the cable conductor is schematically presented in figure 1. In the following the self and mutual inductance of layers are determined per unit length conductor (also see [25]). The thickness of the individual layer is regarded infinitesimal. Furthermore the winding with discrete tapes is approximated by a continuos current sheet.

3.1.1 Layer self inductances

For a single layer configuration the magnetic flux density B, is deduced by the use of Ampere's law, to the following (14) and (15). (14) applies for $r<r_i$, where there is an axial field and (15) for $r>r_i$, where there is a tangential field.

(14) $$B_{inner} = \frac{\mu_0 \cdot I}{L_{pi}} \qquad \text{for } r<r_i$$

(15) $$B_{outer} = \frac{\mu_0 \cdot I}{2 \cdot \pi \cdot r_i} \qquad \text{for } r>r_i$$

L_{pi} is the winding pitch of the layer given from the winding angle α ($\tan(\alpha)=2\cdot\pi\cdot r_i/L_{pi}$), I is the current through the layer, r_i is the radii of the layer and μ_0 is the vacuum permeability ($4\cdot\pi\cdot10^{-7}$ H/m).
The self inductance is found by calculating the enclosed magnetic field energy, W_m [J/m]. W_m is found by first calculating the magnetic field energy density, w_m [J/m^3], given by

$$w_m = \frac{B^2}{2\cdot\mu_0} \tag{16}$$

Resultantly the magnetic field energy per unit length conductor is given by

$$W_m = \frac{1}{2\cdot\mu_0}\int_0^{r_i}\left(\frac{\mu_0\cdot I}{L_p}\right)^2\cdot 2\cdot\pi\cdot r\cdot dr + \frac{1}{2\cdot\mu_0}\int_{r_i}^{D}\left(\frac{\mu_0\cdot I}{2\cdot\pi\cdot r}\right)^2\cdot 2\cdot\pi\cdot r\cdot dr \tag{17}$$

where the first expression is the field energy per unit length conductor stored in the volume inside the cable conductor. The second expression is the field energy per length conductor stored in the volume outside the cable conductor. D is the distance between the layer and the centre of the return path.
The self inductance, L [H/m], is found from

$$W_m = \frac{1}{2}\cdot L\cdot I^2 \tag{18}$$

leading to:

$$L = \mu_0\cdot\frac{\pi\cdot r_i^2}{L_{pi}^2} + \mu_0\cdot\frac{\ln\left(\frac{D}{r_i}\right)}{2\cdot\pi} \tag{19}$$

3.1.2. Layer mutual inductances

The mutual inductances between an inner layer i and an outer layer j, $M_{i,j}$, can be found by the general expression

$$W_m = \tfrac{1}{2}\cdot L_i\cdot I_i^2 + \tfrac{1}{2}\cdot L_j\cdot I_j^2 + M_{i,j}\cdot I_i\cdot I_j \tag{20}$$

where L_i and L_j are the self inductance of layer i and j. I_i and I_j are the currents in layer i and j.
The total enclosed magnetic field energy, W_m, is the sum of three contributions: The energy stored in the volume inside the two layers, W_{mi}, the energy stored in the volume between

the layers, W_{mb}, and the energy stored in the volume from the outer layer to the return path, W_{mo}. The energy stored within each layer is neglected, as the layer thickness is regarded infinitesimal.
By the use of Ampere's law the stored energy is found as before:

$$(21) \quad W_{mi} = \frac{1}{2 \cdot \mu_0} \int_0^{r_i} \left[a_i \frac{\mu_0 \cdot I_i}{L_{pi}} + a_j \frac{\mu_0 \cdot I_j}{L_{pj}} \right]^2 \cdot 2 \cdot \pi \cdot r \cdot dr$$

$$(22) \quad W_{mb} = \frac{1}{2 \cdot \mu_0} \int_{r_i}^{r_j} \left[\left(\frac{\mu_0 \cdot I_i}{2 \cdot \pi \cdot r} \right)^2 + \left(\frac{\mu_0 \cdot I_j}{L_{pj}} \right)^2 \right] \cdot 2 \cdot \pi \cdot r \cdot dr$$

$$(23) \quad W_{mo} = \frac{1}{2 \cdot \mu_0} \int_{r_j}^{D} \left[\frac{\mu_0 \cdot (I_i + I_j)}{2 \cdot \pi \cdot r} \right]^2 \cdot 2 \cdot \pi \cdot r \cdot dr$$

where a_i and a_j are constants (+1 or -1) taking into account the relative winding directions. If the two layers are wound in the same direction around the former the sign of the constants are the same. In the case of opposing twist the constants are each others negation.
The total magnetic energy is given by

$$(24) \quad W_m = W_{mi} + W_{mb} + W_{mo}$$

The mutual inductance between layer *i* and *j* can be calculated by the use of (21) through (24). In the situation where the layers are considered of infinitesimal thickness the mutual inductances per unit length conductor are given by

$$(25) \quad M_{i,j} = M_{j,i} = \frac{a_i \cdot a_j \cdot \mu_0}{L_{pi} \cdot L_{pj}} \cdot \pi \cdot r_i^2 + \frac{\mu_0}{2 \cdot \pi} \ln\left(\frac{D}{r_j} \right) \qquad \text{for } r_j > r_i$$

3.2 Current Distribution

The current distribution in power cables is governed by various parameters:

- the self and mutual inductance of the superconducting layers,
- the joint resistances of the strands and conductors used,
- the usually highly non-linear current – voltage characteristic of the conductor.

Which parameter will be the dominant one will in general depend on what the operating current in relation to the critical current of the conductor is. The current distribution and its dependence on operating conditions will ultimately determine the ac loss that the cable produces (also see [26]).
The calculation involves using the layer self and mutual inductances L_i and M_{ij}, respectively. The layers are considered as being in parallel electrically. Current transfer

between layers is only allowed at the ends of the cable. The voltages V_i and currents I_i in each layer are then governed by the following equation

$$(26)\qquad \begin{pmatrix} V_1 \\ .. \\ .. \\ V_n \end{pmatrix} = \begin{pmatrix} L_1 & M_{12} & .. & M_{1n} \\ M_{21} & L_2 & .. & .. \\ .. & .. & .. & .. \\ M_{n1} & .. & .. & L_n \end{pmatrix} \begin{pmatrix} \dot{I}_1 \\ .. \\ .. \\ \dot{I}_n \end{pmatrix} + \begin{pmatrix} R_1(I_1) & .. & .. & 0 \\ .. & .. & .. & .. \\ .. & .. & .. & .. \\ 0 & .. & .. & R_n(I_n) \end{pmatrix} \begin{pmatrix} I_1 \\ .. \\ .. \\ I_n \end{pmatrix}$$

If all of the voltages and currents are of sine shape (which occurs when all layer currents are below the layer critical current) then this equation can be expressed in complex notation [25,27] as

$$(27)\qquad \begin{bmatrix} V_1 \\ V_2 \\ \vdots \\ V_n \end{bmatrix} = j\cdot\omega \cdot \begin{bmatrix} L_1 + \frac{R_1}{j\cdot\omega} & M_{1,2} & \cdots & M_{1,n} \\ M_{2,1} & L_2 + \frac{R_2}{j\cdot\omega} & \cdots & M_{2,n} \\ \vdots & \vdots & \ddots & \vdots \\ M_{n,1} & M_{n,2} & \cdots & L_n + \frac{R_n}{j\cdot\omega} \end{bmatrix} \cdot \begin{bmatrix} I_1 \\ I_2 \\ \vdots \\ I_n \end{bmatrix}$$

The R_i term in equ. 26 and 27 takes the joint resistance and the AC-loss of the individual layer into account, ω is the angular frequency ($2\cdot\pi\cdot f$) and j is the imaginary unit.
Here $M_{ij}=M_{ji}$ is the mutual inductance between layers i and j,, L_i is the self inductance of layer i. Both inductances depend on the layer radii r_i and the winding pitch L_{pi} .V_i is the voltage and $\dot{I}_i$ is the time derivative of the current I_i in each layer. For a long cable (no contact resistance) the resistive term $R_i(I_i)$ is usually given by

$$(28)\qquad R_i(I_i) = \text{const}\ \text{sign}(I_i)\frac{|I_i|^{n-1}}{I_{ci}^{\,n}}$$

where I_{ci} is the layer critical current. Practically the constant is equal to 1 μV/cm times the length of the cable. The inclusion of the sign term ensures that the resistive part of the layer voltage becomes negative if the current is negative. The overall current is given by

$$(29)\qquad I = \Sigma I_i$$

and the cable critical current is

$$(30)\qquad I_c^c = \sum I_{ci}$$

Since the layers are connected in parallel all the voltages V_i are identical, resulting in a set of layer current values I_i for a given configuration. However, equation 26 does not have a simple general solution due to the current dependent resistive term.

3.2.1 All Layer currents $I_i<I_{ci}$

For very large values of $n \rightarrow \infty$ the second term in equation 26 can be dropped for $I_i<I_{ci}$. In this case it is more useful to invert equation 26 and write it in a differential form. This leads to

$$(31) \qquad \begin{pmatrix} \Delta I_1 \\ .. \\ .. \\ \Delta I_n \end{pmatrix} = \begin{pmatrix} L_1 & M_{12} & .. & M_{1n} \\ M_{21} & L_2 & .. & .. \\ .. & .. & .. & .. \\ M_{n1} & .. & .. & L_n \end{pmatrix}^{-1} \begin{pmatrix} V_1 \\ .. \\ .. \\ V_n \end{pmatrix} \Delta t$$

Thus for each time step Δt the change ΔI_i of the current in layer i is given by equation 31. The total layer current is always

$$(32) \qquad I_i = \sum_{t=0}^{t} \Delta I_i$$

As the total current I is imposed on the cable, we always have $I = \Sigma I_i$, and therefore also

$$(33) \qquad dI/dt = \Sigma dI_i/dt.$$

Equation 31 (or for sinussoidal wave shape, equ. 27 and its inversion) holds if all of the layer currents I_i are below the critical layer current I_{ci}. In this case the layer currents follow the wave shape of the external current with a proportionality factor determined by the matrix in equation 31.

3.2.2 Layer current saturation $I_i \geq I_{ci}$

If the critical current of a layer is reached, its current I_i can no longer increase (or decrease if $I_i = - I_{ci}$). Then, for $R_i >> L_i \, dI_i/dt$ the voltage V_i in equation 26 is now produced by the resistive term and the inductive term $L_i \, dI_i/dt = 0$ can be neglected (ideally because dI_i/dt becomes zero in case of a sharp resistive transition with $n \rightarrow \infty$). Therefore equation 31 is no longer sufficient to describe the system, since $\Delta I_i=0$ is required in this case. If $dI_i/dt=0$, then of course all terms that contain dI_i/dt become zero. Therefore an approximate solution of the problem can be obtained by solving the following sub-problem, for example if layer 1 is saturated

(34)
$$\begin{pmatrix} \ddot{A}I_2 \\ .. \\ .. \\ \ddot{A}I_n \end{pmatrix} = \begin{pmatrix} L_2 & M_{23} & .. & M_{2n} \\ M_{32} & L_3 & .. & .. \\ .. & .. & .. & .. \\ M_{n2} & .. & .. & L_n \end{pmatrix}^{-1} \begin{pmatrix} V_2 \\ .. \\ .. \\ V_n \end{pmatrix} \ddot{A}t$$

where the saturated layer i=1 is removed from the problem by reducing the dimension of the matrix by one: the corresponding row and column is cut out.
This now produces a new distribution of the dI_i/dt, the sum of which still has to equal the external current change dI/dt applied to the system. The difference to before saturation is that the layer i no longer contributes to the overall current changes, since I_i=+/-I_{ci}. In other words, the extra current $\Delta I=dI/dt\ \Delta t$ is now distributed between i-1 layers. This continues until the next layer j saturates. Now two layers (i and j) carry the critical current, and columns and rows j are removed from the matrix, reducing its dimension by one again. This procedure successively continues until all of the layers are saturated, and the cable has reached its critical current.
Evidently this introduces non-linearity into the problem. There is now a 'phase lag' between saturated and non-saturated layers, and the local flux in the cable becomes non-sinusoidal, even if the total applied current has the sine shape.
In order to be able to more specifically describe the effect of saturation we assume that the imposed current I follows a saw-tooth shape of the frequency f. The maximum current is I_0 which decreases linearly to $-I_0$ in a half period. The external voltage switches polarity every half cycle. If the cable inductance was constant over the cycle (it is not) the voltage wave form was rectangular. Now several different cases must be distinguished.

1. The very first up ¼ cycle. The total current starts from zero to increase to I_0. Depending on the inductance matrix both positive and negative values of the layer currents are allowed. As the first layer saturates the inductance matrix is modified according to the rules given above. At I_0 = cable I_c value all layer currents are positive, regardless of the inductance matrix.
2. The first down ½ cycle. The cable current runs from I_0 to $-I_0$. This corresponds to the periodic case – this happens every time the current has reached its maximum. Now - depending on the size of the current I_i with respect to I_{ci} – several cases must be distinguished:
   a) All $I_i<I_{ci}$. If the inductance matrix produces only positive currents for positive voltage then saturation of a layer never occurs because all the layer currents decrease along with the external current.
   b) Some or all $I_i=I_{ci}$. If the inductance matrix only produces positive currents for positive voltage then the saturation condition is immediately relieved as soon as I begins to decrease. Saturation will reoccur as $-I_0$ is approached.
   c) Some or all $I_i=I_{ci}$. If the inductance matrix produces negative currents for positive voltage (inverse condition) then the saturation condition may not immediately relieved as I begins to decrease. Those layers that carry I_{ci} and also have the inverse condition remain saturated until sufficient current has re-diffused into the other

layers, relieving the inverse condition. Then saturation will again reoccur as $-I_0$ is approached.

3. The next up ½ cycle. The cable current runs from $-I_0$ to I_0. This corresponds to the periodic case and the currents are the inverse of case 2.

3.2.3 General case

For the small n values typically found in high T_c superconducting tape conductors (around 20 or smaller) a general solution of the equation 26 has to be found. This can be done by using standard numerical integration techniques or packages. One example is given below.

3.3 Ac Loss

The loss in a superconducting power cable has a number of sources:

1. The cryogenic or cooling loss. This is the loss that is generated by the need to cool the superconductor to below its critical temperature.
2. The eddy current loss in the metallic parts surrounding the superconductor that carries the current.
3. Hysteresis losses in the superconductor itself.
4. Dielectric losses.

A superconducting cable carrying a dc has no eddy current losses. Depending on the level of current and the current voltage characteristics of the superconductor some loss will also occur in it, even though an ideal superconductor transports a dc without loss.
A large amount of work has been carried out on current distributions and ac losses in superconducting cables [28]. However, most of this work has relevance to cables used to wind magnets, being exposed to a significant external magnetic field. The ac loss of power transmission cables has recently become the focus of attention in connection with the high temperature superconductors [1-7]. Transmission cables are only subject to their own magnetic field, rather than an external one. Within the cable, the current distributes according to the cable self and mutual inductances, usually not homogeneously (see above). It has been realised that low loss is obtained with homogeneous current distribution [2], but expressions for obtaining the loss are missing to date.
In this section the results on the current distribution developed above is used to develop a model that computes ac losses for currents up to the cable critical current. Currently not included are current redistributions within one layer and the effect of a gap between tapes in a single layer.

The problem of calculating the ac loss is separated into two sub problems, namely 1) the case when the peak current in each layer is below its critical current, and 2) one or more of the layers have reached their critical current. If $n = \infty$ (where n is the exponent in equation

28) the two contributions can be computed separately, and then – in an engineering like approximation - added up.

3.3.1 $I_i<I_{ci}$ for all layers

In the low current regime none of the layers of the cable is saturated. All of the layer currents are below their respective critical currents. Thus each layer can be described simply as a current sheet $I_{layer} = I_i \sin(\omega t)$ that has an in phase parallel magnetic field $B = B_{tot} \sin(\omega t)$ applied to it. For $n=\infty$ this magnetisation loss P_{mag} per cycle per volume V is simply given by the equations 5-7.
These losses are referred to as magnetisation losses. Hereby P_{mag} is the total power loss, $i=I_i/I_{ci}$, $\beta=B_{tot}/B_p$, and $B_p=I_{ci}/(4\pi r_i)$, where r_i is the median radius of the i-th layer. The total magnetic field perpendicular to the current that the layer sees is given by

$$B_{tot} = \mu_0 \left(H_{ji} \cos\alpha_i + H_{ai} \sin\alpha_i \right) \tag{35}$$

Here α_i is the lay angle of layer i, $H_{\varphi t}$ is the tangential magnetic field, and H_{ai} the axial magnetic field that the layer i experiences due to the other layers. These magnetic fields and the lay angle are given by

$$\alpha_i = \mathrm{ArcTan}\left(\frac{2\pi\delta_i}{l_{pi}} \right) \tag{36}$$

$$H_{ji} = \sum_{j=i+1}^{n} \frac{I_j}{2\pi\delta_i} \tag{37}$$

$$H_{ai} = \sum_{j=1}^{i-1} \frac{I_j}{l_{pj}} \tag{38}$$

This magnetisation loss has a power 3 dependence on both current and magnetic field in the validity range of equation 5 and 6, and a linear dependence for magnetic fields in the range of equation 7.
The total loss in the cable is obtained by summing up the losses in each layer, taking into account that the coverage of the layer with superconductor may be less than perfect, since there is always a gap between the tapes that make up a layer. This loss is an equivalent to the more well known UCD loss (uniform current density [2]), except that the current does not necessarily need to be uniform. For layers that do not carry current but are simply exposed to a magnetic field equ. 5 - 7 lead to the standard critical state loss expressions for a superconducting slab in parallel field.
If $n<\infty$ then the above expressions have to be modified accordingly. Typically the loss tends to increase as compared to the Bean ($n=\infty$) case [29].

3.3.2 $I_i>I_{ci}$ in one or more layers

The current in a saturated layer stays constant at the critical current while the magnetic field produced by the other layers increases. This produces losses not included in equations 5-7. These losses can be computed by calculating the layer voltage and current for each time step Δt from I_0 to $-I_0$. This has to be done for the one whole cycle.
For $n=\infty$ (Bean case) the computation of the current distribution has been outlined already above. This procedure determines I_i and dI_i/dt for each layer, and thus in equation 26 all voltages in the non-saturated layers where $R_i=0$ (all the M_{ij} and L_i values are known). The voltage in all of the non-saturated layers is equal, and identical to the external voltage V_0 applied to drive the current. V_0 does, however, change each time a layer saturates. In contrast, in the saturated layers only the voltages from the terms containing $dI_i/dt \neq 0$ can be computed directly. The 'resistive' voltage $I_i R_i$ is not directly determinable: the current I_i is known, but not a priori R_i. However, since all of the layers are connected in parallel all of the layer voltages must be identical. Thus the resistive voltage is simply the difference between V_0 (which is calculated from a non-saturated layer) and the sum of the voltages coming from the non-zero dI_i/dt. This way a complete voltage and current waveform can be computed for an arbitrary external input current wave shape.
For a finite n equation 26 has to be integrated numerically, which also leads to the complete waveforms of current and voltage. In both cases the overall energy loss per length per cycle is then simply obtained by time integration over half a period

$$\frac{P_{sat}}{lf} = 2\sum_{i=1}^{n}\int_{t1}^{t2} V_0(t)I_i(t)dt \qquad (39)$$

where t_1 is the time of maximum, and $t_2 = t_1 + 1/2f$ is the time of following minimum current. Equation 39 has been implemented numerically and is used to calculate the ac loss results in the next section.

Generally speaking the above formalism develops into the monoblock model (see section 2.6) for an infinite number of layers having infinite pitch. In contrast to the magnetisation losses in the previous paragraph these losses should be called saturation losses, since they arise form the current saturation of a layer. Evidently the physical loss mechanism is the same for the two regimes – it is the drag of the moving flux lines. However, in the low current regime (section 3.3.1) they move within a layer, and in the high current regime (section 3.3.2) they move through a layer. Evidently in a cross-over regime both mechanisms occur. In the case of unequal current distribution and high n-value they are most easily distinguished.

3.4. Discussion and Comparison to Experiments

First a general comment to the division of the loss regimes in two. It is clear that the physical mechanism of loss is the movement of flux lines in the superconductor. Thus in principle it is physically not correct to add the two contributions, as they have the same

physical mechanism. However, since the saturation loss is typically much larger than the magnetisation loss, from an engineering point of view in many practical cases it even makes sense to neglect the magnetisation loss at high currents.

In the first example a cable is shown where the current tends to flow towards the outside of the cable. The calculation shows this, and the loss calculated is very similar to the one obtained from the monoblock model. In example 2 only magnetisation loss occurs due to a forced equal (or almost equal) current distribution. A distinction between the two different regimes described here may in fact be not so easily done, in particular if the saturation losses are small and comparable to the magnetisation losses. This is the case in the third example shown here, where a full numerical solution of equ. 26 was carried out using a low n value.

3.4.1 Example 1: 10 layer cable

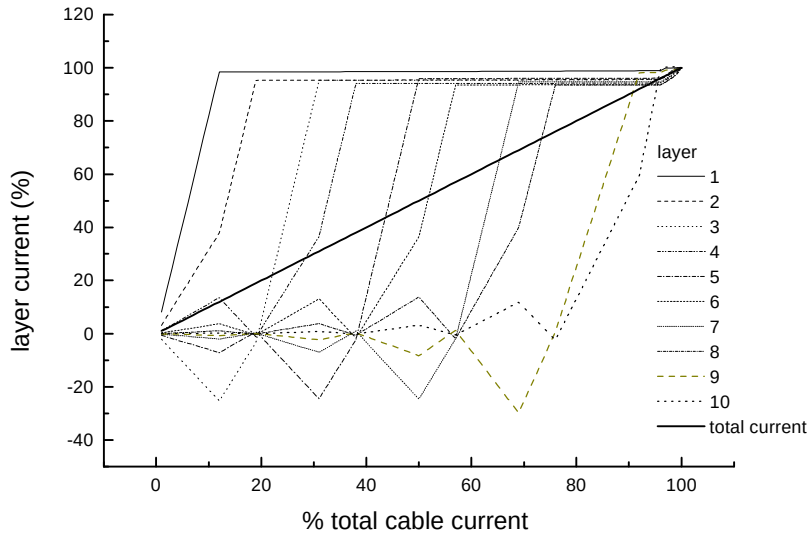

Figure 2. Layer current as function of external current calculated for cable SW3. The fact that layer current saturation does not occur exactly at 100% is due to discretisation in the numerical calculation procedure.

A 10 layer cable with alternating (switching winding direction) but otherwise constant winding pitches is regarded first (Southwire cable #3, from [30]). Shown in figure 2 is the calculated current distribution (layer thickness was estimated from difference between former and outside diameter) as a function of total cable current when the current is first increasing from zero. Initially almost all of the current is concentrated on the outer layer (#1) of the cable. When this layer saturates more current is driven into layer 2, and so on until the cable is completely filled with current. This current saturation of the layers is shown in figure 2. It shows the current in each layer as a function of time for a linearly increasing external current. The external current increases continuously, while the layer currents exhibit discontinuities in the slope whenever a layer reaches its critical current.

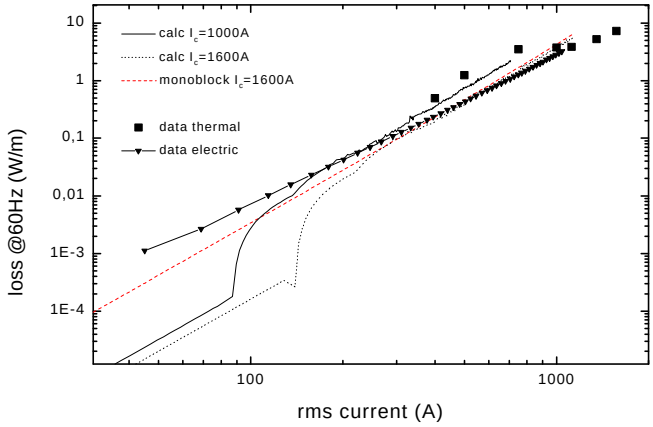

Figure 3. Calculated and measured losses in cable model SW3.

This is a result of the fact that the current supplied to the cable has to be distributed to one layer less, thus increasing the $|dI_i/dt|$ of all layers.
The corresponding losses at 77K have been calculated and are shown in figure 3 together with data taken from ref. [30]. It should be noted that the original critical current of the cable model was given as 1600A, whereas it had degraded down to a critical current of 1000A (all dc, 1μV/cm) by the time the electrical loss measurement was carried out. The agreement between calculation and loss is quite good, but not perfect. In particular at low currents below the saturation of the first layer the measured loss is significantly underestimated. For high current the calculated loss is similar in magnitude to the monoblock loss, but with a slightly lower power exponent (n=2.86). Experimental losses appear to be of the same order of magnitude as the calculated ones, but have a even lower power exponent (n=2.63) than the current calculation and the monoblock model (n=3). Better agreement could have been obtained by using the critical current as fitting parameter. It can also be seen that the magnetisation losses (if extrapolated from below 150A to higher currents) are at least one order of magnitude smaller than the saturation losses.

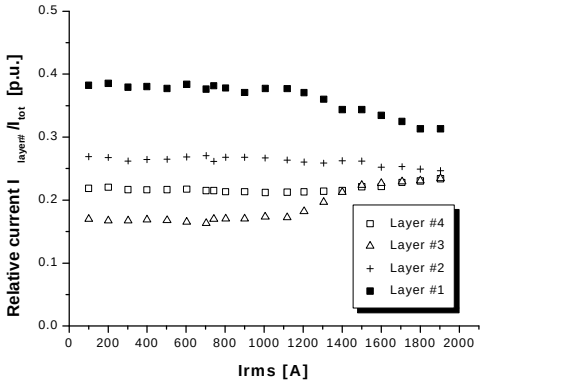

Figure 4. Measured relative current vs. total current.

3.4.2 Example 2: Four layer cable

This cable is a 3m long cable model that has 4 layers with alternating pitch of 0.3m, wound at the Technical University [25]. Current was fed into each layer separately which introduces resistance into the current path that tends to equalise current distributions. The DC characteristics of the cable conductor has also been investigated but is not considered here.
The current in the individual layer has been monitored with torroidal Rogowski coils placed around layer 4 (inner layer), layer 3 and 2 and so forth. The measured current distribution as a function of the total current at 50 Hz is shown in figure 4. In Table 1 the calculated current distribution is shown in two cases; with and without joint resistances.

The current distributions are calculated by the use of equ.27 where the inductances are scaled with the length of the cable conductor. The current distribution calculated without regard to joint resistances corresponds to a long cable conductor, e.g. the case we want to investigate. It is noticed that in this case a current is induced in layer 2 which actually is running backwards! The calculation is in both cases only valid for low currents where the AC-loss are negligible:

(40) $R_i = R_{joint,i}$ for $I \ll I_C$

Layer #	R_{joint} [μΩ] measured @ 50 Hz	Calculated layer current for $R_i = R_{joint,i}$ I_{layer}/I_{tot} [p.u.]	Calculated layer current for $R_i = 0$ I_{layer}/I_{tot} , [p.u.]
4	17.2	0.20	0.06
3	18.0	0.13	-0.19
2	17.6	0.27	0.43
1	13.5	0.40	0.70

Table 1. Calculated current distributions. The joint resistances are measured.

Good agreement is found between calculated and measured current distribution for currents lower than 1000 A_{rms}. At 1000 A_{rms} the current begin to redistribute as the outermost layer is carrying the critical current. It appears that the measured current distribution between layers is substantially more uniform than the case would have been with smaller joint resistances or with a longer cable conductor. Figure 5 shows the measured loss at 77K in the case where these series resistances are present. Thus over almost the whole range of current shown in the figure the measurements really should reflect the magnetisation loss occurring in the cable. The calculated curve thus contains only the magnetisation loss up to about 1000A. Also shown is the loss curve for equal current distribution. The agreement between measured and calculated loss is quite good in the low current regime. For currents higher than about 600A rms. the measured losses are higher than the predicted ones, indicating that some current redistribution or saturation occurs, possibly even among tapes in a layer.

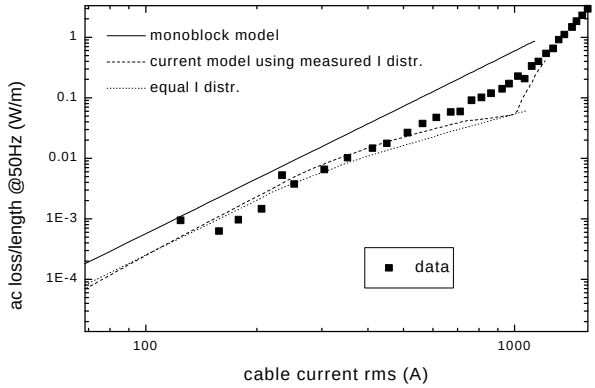

Figure 5. Comparison of calculated and measured ac loss for 4 layer cable model.

3.4.3 Example 3: Eight layer cable

This cable is a 10 m long 8 layer cable that was constructed with the intention of having equal or close to equal current distribution using a specific winding pattern [31]. The ac loss data at 77K is shown in figure 6, together with the theoretical curves calculated using a full solution of equation 26. The measured transport critical current (3240A at 1μV/cm) was used for the loss calculation under the assumption that the critical current of all layers is

equal. A power exponent of n=8 (measured value for the tapes) was used for the saturation loss curve. Also shown is the curve for equal current in all layers, in which case only magnetisation loss is produced. The match between calculation and data is very good. The cross-over of the magnetisation and saturation losses occur at around 1700A. At high currents it can be seen that the magnetisation loss becomes linear with current, while the saturation loss increases quite rapidly and dominates. The experiment shows (and theory predicts) that the magnetisation loss at low currents follows the I^3 behaviour, switching to a lower exponent for higher currents. However, the calculated magnetisation loss at low current is larger than the measured one (about a factor of 3 at 300A), and the transition from power 3 to power 1 in the calculated curve occurs at a lower current than predicted. This may indicate granular effects, as the local current density could be higher than the transport one used here, lowering magnetisation losses and pushing the transition point to higher currents. It should also be noted, though, that the error bars on the losses at low currents are quite large due to the fact that resistive joint contributions have been subtracted.

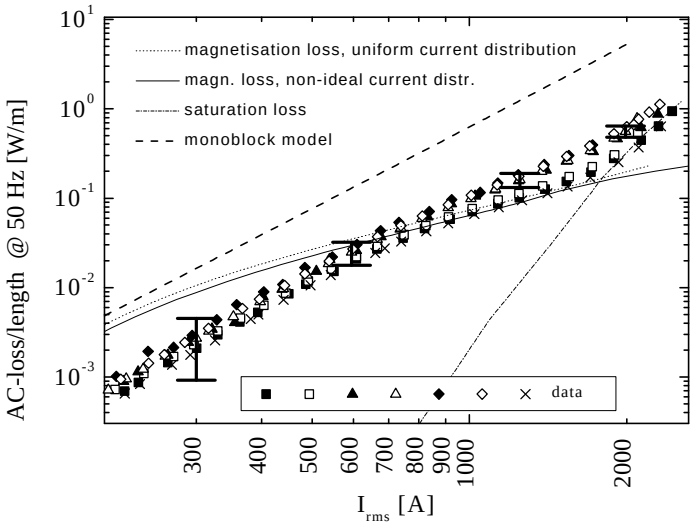

Figure 6. Comparison of calculated and measured ac loss for 8 layer cable model.

3.5 The ac loss due to eddy currents in the metallic parts of a superconducting cable

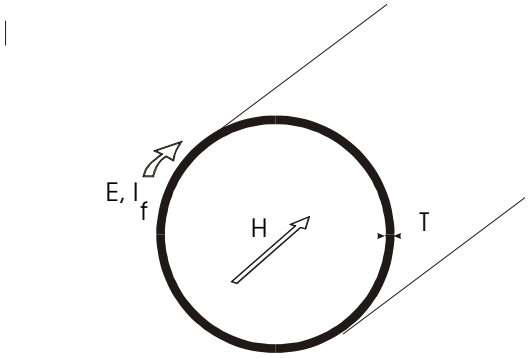

Figure 7. Geometry of eddy current in former.

The ac losses occurring in the metallic parts of a single phase cable are evaluated. There are tree principal contributions: the former tube carrying the superconducting tapes, the outside vacuum vessel, and the silver tapes containing the superconductor. In case of the use of pure metals like Al or Cu the losses in the former can be a significant contribution to the overall losses of the cable. Ac losses in the outside vacuum tube are negligible. The eddy losses in the silver tapes are small, as long as they are isolated from each other (including layer isolation).

3.5.1. Former

A loss will develop in the former due to ac eddy currents that are generated in it due to the presence of a magnetic field arising from currents within the superconductor. The former sits inside of the superconducting winding, acting as the secondary winding of a transformer, the primary of which is the superconductor. In figure 7 the geometry of the problem is described. For the rest of the calculation we assume T<<R, and skin depth=∞.
The superconductor in the i th layer (for simplicity only one layer is shown) produces in its center the axial homogeneous magnetic field

(41) $$H_i = \frac{I_i}{L^i_p}$$

parallel to the y direction. Here $I_i=I_{io}\sin(\omega t)$ is the current in the i th layer with a twist pitch L^i_p ($\omega=2\pi f$, f=50Hz). The twist pitch must be associated with a sign according to the helicity of the winding, positive for clockwise, and negative for counterclockwise winding. Due to the length of the solenoid (the cable) the layer diameter does not enter the magnetic field generated. The field H responsible for ac loss in the former is

(42) $$H' = \sum_i H_i \qquad \text{and} \qquad H = H'/\sin(\omega t)$$

This field is zero, if each layer has a counterpart with opposite helicity, assuming equal currents in both. In general this is not the case (see above). As the current distribution between layers may also change as a function of total current in the cable the loss in the former may well be a non-monotonic function of the total cable current with one or more maxima. Changes in the layer current distribution due to the mutual inductance between the former and the layers should be expected, and must be looked at in further work.
The induced electric field E is acting along the former circumference. The voltage U_{ind}

(43) $$U_{ind} = \oint dE = \frac{\partial \Phi}{\partial t} = \mu_0 \pi R^2 \omega H \cos\omega t$$

is generated along the circumference and is induced by the change of flux ϕ inside the former. Its peak value U_{ind}^m is given by the terms in front of the cosine. The peak value of current in the former is given by

(44) $$I_f^m = U_{ind}^m / R_e$$

where R_e is the electrical resistance of the former for current flow along the circumference. For a given former length l and a resistivity ρ we find $R_e = \rho\, l'/A$, where A=l*T and $l'=2\pi R$. Here T is the former thickness.
Thus the induced current in the former becomes

(45) $$I_f^m = \frac{\mu_0 R \omega T l}{2\rho} H$$

The effective power loss per length is then given by

(46) $P_f = ½\ U_{ind}^m\ I_f^m/l$

which results in

(47) $$\frac{P_f}{l} = \frac{ì\ ^2_0ð\ ^3R\ ^3f\ ^2T}{ñ} H^2$$

There is a very strong (cubic) dependence on the former radius, while the thickness enters only linearly. Materials with high resistivity ρ are preferable.
As example materials for the former we consider pure Cu (or pure Al, which has almost identical resistivity), and non-magnetic stainless steel (SS). Resitivities at 77K are 0.21 (Cu), 0.25 (Al) and approximately 70 μΩcm (SS). In practice it is recommended to actually measure the resistivity (77K) of the former used, and use that resistivity in equation 47. This is in particular important for the pure materials, since small additions of impurities can significantly change the resistivity at 77K. In practice losses of about 1W/m are obtained for a 1 mm thick Cu former of 30mm diameter in a field of 1000 A/m. Thus if there is a magnetic field at the former Cu should not be used as a material. It should be noted that the skin effect would tend to lower losses, so that equation 47 is to be regarded as an upper limit (see [32]). For formers made of braided materials the losses are expected to be much lower, as the resistance between the braids must be overcome by the induced currents.

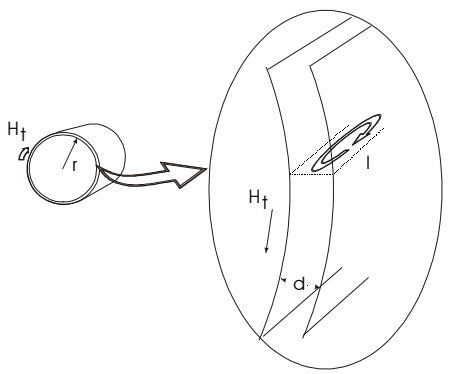

Figure 8. Geometry of outer tube. The former, the tapes and insulation are not shown.

3.5.2. Vacuum Tube

The geometry is given in figure 8. The situation is different from the former, as the magnetic field is now tangential to the tube, depending on the total current I_t in the cable as

(48) $$H_t = \frac{I}{2ð\ r}$$

The current distribution in the layers does not matter. The induced current is now flowing along the length l of the sheath with opposite polarity on the inside and outside. The flux change driving the eddy current is occurring in the area d times l, and is thus significantly smaller than for the former. In order to simplify the calculation a constant value (in fact the maximum value) for the induced voltage is used, stemming from the use of the borders of the area d times l only. This approximation will lead to an overestimation of the losses as the real induced voltage varies with position in the loop. The calculation proceeds in a similar manner as above, leading to

(49) $$\frac{P_v}{l} = \frac{\mu_0^2 \omega^2 f^2 d^3}{2\pi\rho} I_t^2$$

In this case it suffices to give one numerical value. As example (worst case) we take: stainless steel as material (thus ρ=70$\mu\Omega$cm), d=0.2mm, I_t= 2000A, ν=50Hz, r=0.04m. For these values the power loss per length is 7.1×10^{-6} W/m, thus completely negligible compared to the losses in the superconductor or the possible losses in the former. Even if pure Cu tubing of 0.4mm thickness was used, the losses would merely grow to a value of order 0.01 W/m, still very small. A corrugated tube would show losses that are slightly higher than those given here due to the fact that there is more material per length of tube compared to a smooth one. Thus losses higher by a factor of 2 or 3 can be expected.

3.5.3 Superconducting tape / silver matrix

A silver tape (containing the superconductor) experiences both radial and axial magnetic fields, depending on in which layer it is situated. The currents that can flow depend now on the tape and layer insulation.

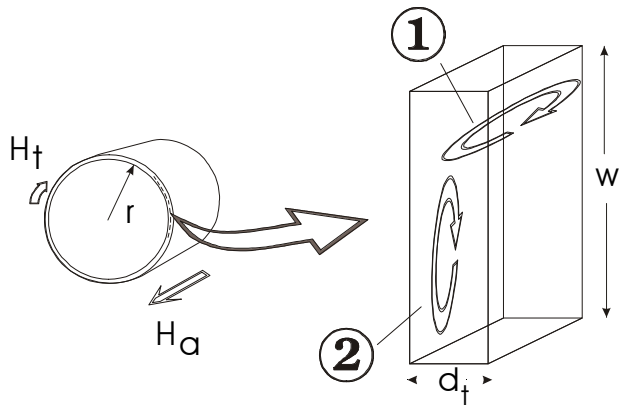

Figure 9. The geometry of isolated tapes experiencing both tangential and axial magnetic fields. On the right a single tape is shown. The transport current is parallel to H_a. Induced current system 1 is due to the tangential, system 2 due to axial magnetic field.

If there is neither tape nor layer insulation the tapes touch each other, and current can circulate around the circumference of the layer. Thus the situation for the inner layers is similar to that of the former, being exposed to the axial field created by currents in the outer layers. Thus the loss would be of similar magnitude as for the Cu former shown in figure 7, and equation 47 can be used to get a rough loss estimate, calculating H from the total current I_t. The loss would be expected to be proportional to I_t^2. Indeed this behaviour is experimentally found in a number of studies.

If the layers would be isolated from each other, then the length scale for currents would depend on whether the tapes in one layer touch themselves or not. If they do, then again currents around the circumference are possible, depending on the frequency with which these touches occur. A loss calculation would be difficult in this case. If the tapes do not touch then the situation is identical to the one for isolated tapes (see below).

If the tapes themselves are isolated from each other, then only local eddy currents in each tape are possible. Both the axial and the tangential field induce currents, as shown in figure

9. For simplicity the effect of the lay angle is neglected. This can be done because the currents are local, and the tapes are not electrically connected.
The ac loss now has two components. For the loss caused by the tangential field in one layer we can use directly equation 49, putting the layer radius as r, and using the tape thickness d_t. Using the parameters from the previous section with the resistivity of silver (ρ_{Ag}=0.3μΩcm) one arrives at a power loss of about $3x10^{-3}$ W/m per layer (worst case).
In order to evaluate the loss due to the axial magnetic field we have to modify equation 47 to account for the rectangular shape of the tape. This leads to

$$(50) \qquad \frac{P_{Ag}}{l} = N\frac{\mu_0^2 \pi^2 d_t^3 f^2 w^2}{\rho_{Ag}(w+d_t)} H_a^2$$

Here N is the number of tapes. Again an approximation was used for the induced voltage, taking the maximum value at the outer perimeter of the tape, leading to an overestimation of the losses. If typical tape dimensions are inserted into equ.10 (tape width 3mm, tape thickness 0.2mm, ρ_{Ag}=0.3μΩcm, $H_a=10^4$ A/m, N=33/layer) the loss due to eddy currents in the silver is 10^{-3} W/m/layer. This estimate is a worst case, because it assumes that all tapes are exposed to the full magnetic field produced at 2kA, which is not the case.
Thus the total loss due to eddy currents in the silver for insulated tapes is expected to be less than $4x10^{-3}$ W/m/layer at a current of 2kA in the cable. Since this loss value for isolated tapes are rather small, a more exact calculation is not deemed necessary at this point.

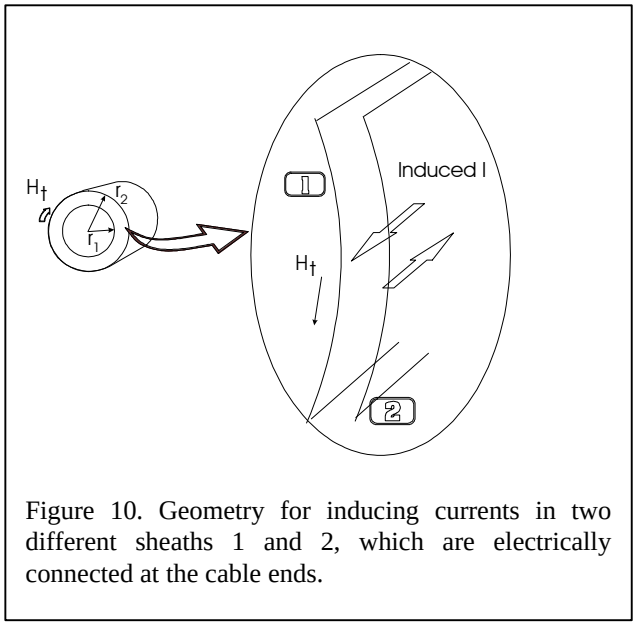

Figure 10. Geometry for inducing currents in two different sheaths 1 and 2, which are electrically connected at the cable ends.

3.5.4 Ac loss in case of a conducting connection between sheaths

However, a large loss can arise if there is an electrical connection between sheaths at the ends of the cable, for example the former and the inner wall of the cryostat, or the inner and outer wall of the cryostat (see figure 10). This problem is known also in conventional cables [33]. The loss is due to the tangential magnetic field H_t caused by the total transport current I of the cable. This magnetic field is always present independent of the winding pattern of the layers. Unlike the loss caused in one sheath alone the flux enclosed between two sheaths is much larger, and a large loss is expected.
Let the cable carry a total current of I_0 at its peak at the frequency f. The power loss in two sheaths with radii r_i, wall thicknesses $t_i << r_i$ and resistivities ρ_i is approximately given by

(51) $$\frac{P_{s1s2}}{l} = \frac{\delta\mu_0^2 I_0^2 f^2}{\frac{\rho_1}{t_1 r_1} + \frac{\rho_2}{t_2 r_2}} \ln\left(\frac{r_2}{r_1}\right)$$

Hereby it is assumed that $r_2 > r_1$, and that the cable transport current flows inside of sheath 1. If sheath 1 is to be the former, a good approximation for r_1 would be the layer radius of the winding. The skin effect is not taken into account, and it doesn't need to be (see below). If this loss is calculated for an inner sheath (for example the former) of 30mm diameter, and an outer sheath of 50mm diameter, both 1mm thick and made of stainless steel (high resistivity of 70μΩcm), then the resulting power loss is about 0.34W/m, a large loss comparable in magnitude to thermal losses and losses in the superconductor! Other examples could be given, but the conclusion is quite evident: there must not be a metallic connection between the different sheaths of the cable at the ends, to be exact at both ends. Welding or soldering at one termination is allowed, as the current circulation is interrupted that way.

3.6 Ac loss measuring methods

The measurement of ac losses in superconducting cables is complicated, which is why there have been several methods developed to achieve this goal.
In the thermal method the heat created by the loss is used to determine the power loss. This can be done by measuring the gaseous boiloff of the liquid cryogen - liquid helium or nitrogen - used. Hereby the operating temperature of the cable is very close to that of the surrounding liquid. The sensitivity of this method in particular in liquid nitrogen is poor since the losses and boiloff are small; measurements on cables have been performed [34] using this method. If the cable is thermally insulated from the liquid then the loss can be measured directly by placing thermometers along the cable that measure the temperature increase caused by the losses [7,35,36]. Critical is the thermal insulation which can be achieved using vacuum or some insulating substance. The thermal methods work well and give true ac losses, but tend to be very tedious to use.
In the electrical four probe method the voltage in phase with the current is directly measured and multiplied with the current to give the power loss [1-6]. The problem with this method is that the inductive (out of phase) components of the measured voltage is much larger (100 to 1000 times) than the resistive component. This creates the need for compensation and very accurate phase angle measurements. Furthermore, induced voltages from other parts of the circuit may falsify the measurements, in particular in three phase configurations.
There also is a third method, the resonant current experiment (RESCUE, [37]). Hereby the superconducting cable whose losses are to be measured is simply short circuited by a capacitor. The circuit thus formed contains an inductor (the cable itself) and a capacitor, and can be made to resonate. Then a resonant current is induced in this circuit, the decay of which is used to determine the losses in the superconducting cable.

3.6.1 Thermal methods

A non-electrical method that is used for determining the ac loss in superconducting cables is the thermal method. In this method the heat developed by the ac loss is measured, usually by measuring a temperature difference between two thermometers. The principle is illustrated in figure 11, shown for the case where the coolant - in most cases liquid nitrogen - is allowed to flow. Hereby two thermometers are needed, located at different positions l_1 and l_2 along the length of the cable. The thermometers then measure the difference in temperature ΔT between the two points, and the ac loss per length P is given by $P = \Delta T\ c\ v\ A/(l_2-l_1)$, where A is the cross section of the cooling channel in which the coolant of heat capacity c is flowing with the velocity v. A variant of this method can be used in stagnant coolant [35], in which case the cable is thermally isolated over a certain stretch, while being cooled elsewhere. One thermometer is then placed there, and another into the coolant. When current is flowing the temperature will increase in the part of the cable that is thermally isolated. Both methods can be calibrated using a dc current in the cable or a heater assembly.

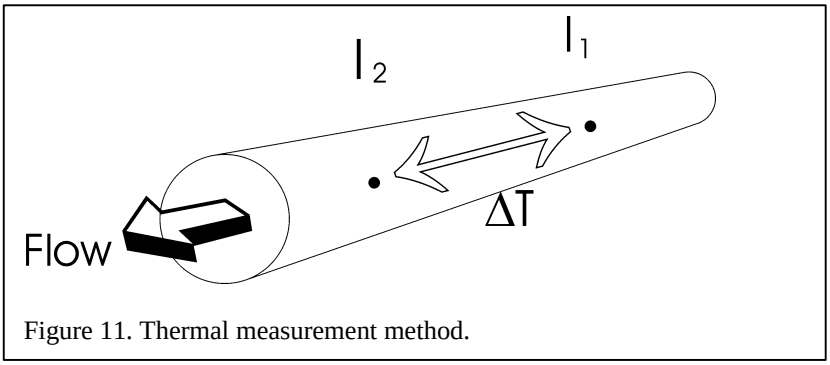

Figure 11. Thermal measurement method.

A third method measures the gas volume evaporated by the heat generated in the cable [34]. This is obviously only usable in a boiling coolant. This method is not very sensitive. The advantages of all thermal measurements are the possibility to measure under conditions where electrical methods are not applicable, for example in three phase conditions, and the possibility to measure when both transport losses and losses due to a magnetic field are present. The general disadvantage is that they are complicated to carry out and can be lengthy, even though only basic quantities are measured. Electrical noise can play a role, and the sensitivity is reduced compared to electrical measurements.

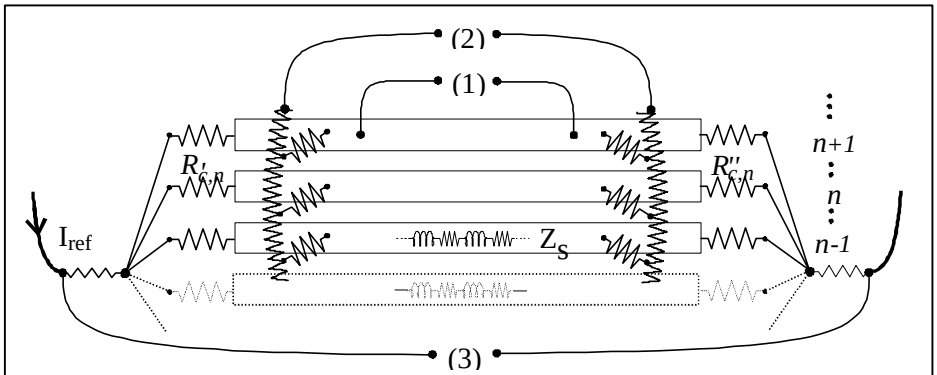

Figure 12. Representation of the connections to the tapes in a one layer cable conductor. Shown are the connection to a single tape (1) and to a ring contact (2) and to the normal metal joints (3).

3.6.2 Electrical Four probe methods

Single layer cable

The high temperature superconducting cable prototypes are generally, irrespective of the actual cable design, based on a centrally located conductor. This conductor consists of superconducting tapes (typically the $Bi_2Sr_2Ca_2Cu_3O_{10+x}$, Ag sheathed tapes) wound spirally around a former. More than one layer of tapes is generally needed in order to obtain a high critical current and sufficiently low ac losses. One important issue when using electrical four probe methods using phase sensitive (lock-in) detection is the choice of potential probe positions. These should be placed in such a way that the true loss can be derived from the measurement. For single layer models these can be placed in at least three ways: (1) directly on a selected tape, (2) on all tapes using ring contacts or (3) on the normal metal current leads. These three ways of placing the voltage probes are illustrated in figure 12. Schematically depicted is a cable conductor where, however, only three tapes are actually shown. The tapes are represented as a series connection of inductors and current dependent resistors. Each tape has in each end a separate contact resistance, $R'_{c,n}$ and $R''_{c,n}$, to the point of current injection. The ring contact is drawn as a spatially extended resistor along which the tapes are connected through individual contact resistances. In order for the single tape contacts (1) to be used successfully, the voltage drop over the probed tape should be representative for the voltage drop over all tapes both in magnitude and in phase angle (with reference to the total current) at the chosen frequency. Obviously this requires that the properties (critical current, position, self and mutual inductance) of the tape itself are representative but it is also required that the contact resistances to the current leads are representative. If these requirements are not fulfilled unrepresentative loss-voltage levels will be measured, or even worse: the current through the tape under consideration might be shifted in phase with respect to the total current resulting in remarkable errors in the phase sensitive detection scheme. The contact resistance (of the order of micro-ohms) becomes important because of the short sample length (i.e. low inductive and resistive voltages over the superconductor). The most common reason for differences in tape quality is degradation due to handling. The requirements to even tape properties and even contact resistances often turn out to be only

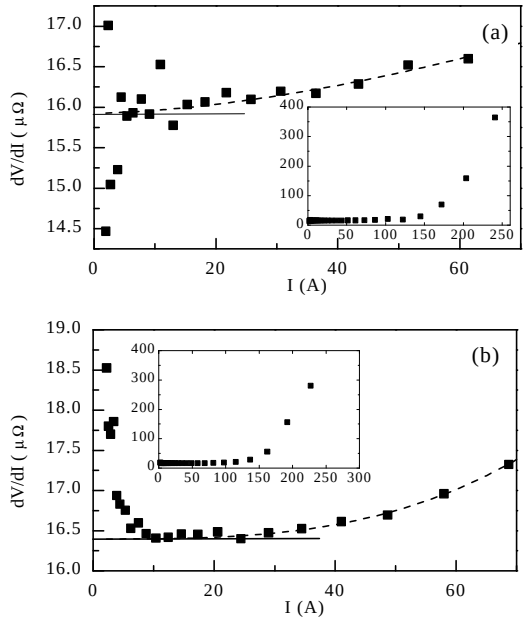

Figure 13. Magnification of the derivative of the in-phase AC-voltage measured at the joints as a function of the total current. (a) as-fabricated conductor with 16 tapes, (b) after controlled damage of 4 tapes. The dashed curves are guides to the eye. The intersection with the ordinate axis gives the effective contact resistance. The inserts show the full data sets.

partially fulfilled resulting in large errors at currents below the critical current. Probing a single tape, only, is thus not a reliable way of measuring. Ideally all the tapes should be probed. It might be anticipated that a ring contact (2) which is connected to all tapes (in a single layer conductor) along the conductor's circumference is an appropriate solution for averaging out differences in voltage. Such a ring contact may work given the ring itself has a resistance (per unit length) which is much smaller than the resistances to all the tapes, effectively yielding a star-configuration. It is also required that the resistances between the ring and the tapes are all of the same size. If the currents that will flow in the ring due to uneven potentials creates voltages along the ring comparable to the voltages over the tapes the measured voltage will depend on where precisely the voltage leads are attached to the ring contact. Therefore a practical ring contact constituted by a wire connected to all tapes of a cable conductor round its circumference either by soldering or by silver paint is not reliable in the general case.

A third way of placing the voltage tabs is to put them on the normal metal joints to which the superconducting tapes are usually soldered at a point where the current density changes linearly with the magnitude of the current. In this case it is reasonable to expect the measurement to be insensitive to the variations in of tape quality and contact resistances. Only one would have to subtract from the measured voltage the ohmic contribution stemming from the effective contact resistance constituted by the resistance of the metallic joints themselves and the resistance of the connections to the tapes. Here we present data that shows that this measurement method works in many cases, but also that it has its limitations.

The data shown in the following were all acquired by measuring the AC-voltage using a lock-in amplifier. The signal used for reference was phase-calibrated against the voltage from a torroidal coil (Rogowski coil) placed around the lead carrying the current to the sample. The uncertainty on the phase determination was less than 0.025°. The current dependent values of the corrected reference phase were used to extract the resistive part of the recorded AC-voltages, i.e. the voltage *in*-phase with the total current. The experimental data shown here are from the measurement of a representative single layer conductor. This sample was made from 16 Bi-2223 HTS tapes placed parallel to the long axis of the former, an Etronax tube with a diameter of 14.5 mm. Full coverage on the surface of the former was achieved. The total length of the superconductor was 118.5 cm. The tapes were soldered on to two short Copper tubes mounted at the ends of he former. The critical current I_c of the sample was measured to 187 A (at 77.3 K, using the 1 μV/cm criterion).

When determining the effective contact resistance of the current joints we have found it useful to calculate and plot the derivative of the in-phase part of the recorded AC voltage, $V^{=}$, as function of the total current I_{tot}. Due to the skin effect it is necessary to determine the contact resistance for each applied frequency, i.e. the DC contact resistance derived from DC current-voltage curves can not be used in the AC case. If the loss component of the superconductor's impedance is denoted $R_s(I)$ and the effective contact resistance R_c , the derivative of the in-phase voltage (i.e. the differential AC-resistance) is given by:

$$\frac{\partial V^{=}}{\partial I} = R_c + R_s(I) + \left(\frac{\partial R_c}{\partial I} + \frac{\partial R_s}{\partial I}\right) \cdot I \qquad (52)$$

Assuming that the AC-losses in the superconductor are very low ($R_s << R_c$) at $I \approx 0$ the contact resistance can derived from a plot of $\P V^{=}/\P I$ versus I as the intersection of the data with the ordinate axis (at I = 0). An example of a recording at 48 Hz is shown in Fig. 13a. The dashed curve, a guide to the eye, indicates the position of the intersection with the ordinate axis. The limiting value for the effective contact resistance is in this case thereby determined to $R_c = 15.92\ \mu\Omega$ with an uncertainty of about $\pm 0.05\ \mu\Omega$. The scatter in the data at currents below 15 A we believe is due to a too low time constant used for the phase sensitive voltage measurement. However, as the results discussed below indicate it could also be due to a re-distribution of the current. In order to systematically investigate the influence of variations in tape quality on the measurements we on purpose buckled 4 of the 16 tapes on the sample cable conductor in one end. From the DC V-I curves we observed a reduction from I_c of 187.0 A to 179.6 A corresponding to a reduction of about 1.8 A for each of the damaged tapes. This is a reasonable value taking the total tape length of 118.5 cm into account. The resulting differential AC-resistance curve equivalent to the one in Fig. 13a is shown in Fig. 13b. The limiting value of the contact resistance is determined to $R_c = 16.42 \pm 0.05\ \mu\Omega$ when extrapolating a smooth curve through the data for currents higher than ≈ 10 A. This value is somewhat higher than for the un-damaged conductor. This may be due to and enhancement of the apparent resistance of the solder-joints caused by a redistributed current flow, i.e. the current in the damaged tapes is fractionally smaller

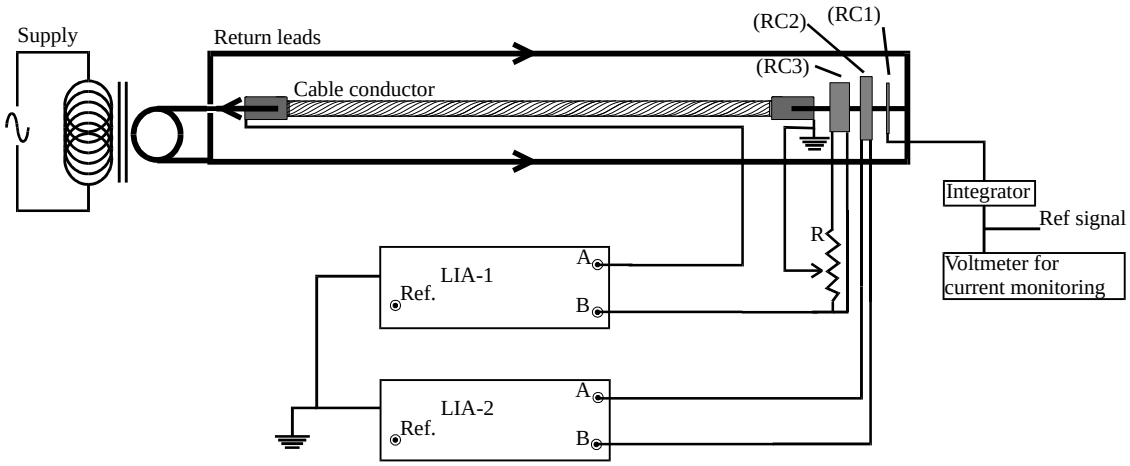

Figure 14. Schematic of the electric circuit for measuring AC-losses in cable conductors. Two lock-in amplifiers measure the cable voltage and the signal from a precision Rogowski coil, RC2. The amplified and integrated signal of Rogowski coil RC1 supplies the lock-ins with a reference signal and is used for current monitoring. An inductive compensation circuit consists of the Rogowski coil, RC3, and a resistive voltage divider, R.

than in the rest of the tapes. Another explanation is that the places where the 4 tapes have been buckled add an ohmic contribution to the measured voltages. We regard the latter explanation as the most plausible also illustrating the weakness with this technique: any ohmic (= resistive and current independent) contribution from the cable conductor itself will be subtracted. Ohmic contributions could originate from eddy current losses in surrounding metal (e.g. in the former) and from coupling losses in the silver matrix of the HTS tapes or if the tapes touch electrically losses from currents flowing from tape to tape

through the silver. In Fig. 13b at currents lower than 10 A the differential resistance is seen to increase rapidly with increasing current. *This* we attribute to a current re-distribution away from an even distribution effectively increasing the joint resistance. A rough estimate of how big an influence it would have if the 4 damaged tapes are without current can be calculated taking the total joint resistance in the undamaged case as $R_c = R_{c,n} / N$, where $R_{c,n}$ is the joint resistance of each tape and N is the number of tapes. This yields $R_{c,n} = 254.7\ \mu\Omega$. If $N = 12$ the result is $R_{c,n}(12) = 21.2\ \mu\Omega$. Though this is a crude estimate it makes sense when compared with Fig. 13b if it is assumed that no current flows in the 4 damaged tapes at very low currents where the resistance of the good tape is practically zero.

Multi layered cable

In multilayered cable conductors generally the tapes at the lower layers are not accessible for voltage measurements. Therefore in the example following all of the contacts have been made on the joints to the layers, also focussing specifically on voltage lead position, phase errors, inductive compensation and location of current return leads. The investigations have been carried out on a 10 m long superconducting cable conductor model containing 8 layers manufactured by NKT. The conductor has been wound on a commercial winding machine, adapted for use with the superconducting Ag-alloy sheathed Bi-2223 tapes. In each end of the cable the superconducting tapes are soldered onto a cylindrical copper joint. The critical current at a voltage criterion of 1μV/cm is 3240 A at 77 K.

The cable conductor was tested immersed in liquid nitrogen (LN_2) in a 10 meter long bath type cryostat made from non-metallic materials. A tight lid was placed over the bath. The liquid nitrogen was replenished automatically when a certain minimum level was reached.
The electrical circuit is shown in figure 14. Current is supplied from a transformer with only one secondary winding (the test circuit itself). The primary winding of this transformer is fed by a variable transformer (not shown) allowing control of the voltage and the current. The variable transformer is connected directly to the grid. Two copper cables placed on each side of the cryostat returns the current to the transformer. In order to detect if the geometry of the current return path has any effect on the measured loss two return lead positions were tested, see figure 15. In both cases the two return leads were separated by a distance of 400 mm and placed with equal distance to the cable conductor. In the (two fold) symmetric case (SYM) the return leads were placed in the same plane as the cable conductor. In the asymmetric case (ASYM) the leads were placed in a plane 140 mm below the conductor.

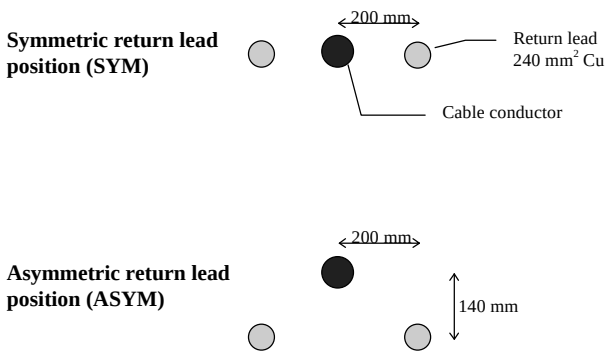

Figure 15. The two configurations of the return leads under investigation.

The voltage taps were placed at the ends of the copper joints. This

position of the voltage taps secures meaningful measurements as the overall voltage is measured avoiding any spurious and current dependent voltages produced by possible current redistribution effects as a function of current in the joints (see above). The measured voltage is thus a sum of the voltage over the superconductor itself and the voltage over the copper joints. The latter contains contributions from the resistance of the copper in the joints and from the contact resistance between the superconducting tapes and the copper. The loss added to the measurement by the joint resistance has to be removed in order to deduce the actual AC-loss of the superconductor. Three sets of voltage leads, L1, L2 and L3, were connected to the voltage taps. The leads were positioned at distances from the conductor of 1 mm, 15 mm and 30 mm, respectively, thus creating three different pick-up loops.

The measurement set-up consists of two identical lock-in amplifiers, LIA-1 and LIA-2, and three torroidal coils (Rogowski coils), RC1, RC2 and RC3. RC1 is a commercial Rogowski coil with an amplifier and an integrator. The high quality output of the integrator of RC1 is used for the current measurement (using a digital AC-voltmeter) and as external reference signal for the two lock-in amplifiers. However, there is a small current dependent phase shift in the output of the integrator. The purpose of RC2 and RC3 is to provide signals which are shifted precisely 90.00° with respect to the current. These signals can then be used to determine the *actual* phase shift of RC1 enabling a post-acquisition correction. Additionally they can be used for inductive compensation. RC2 and RC3 have been produced in the laboratory without any metallic parts other than the wire. The cable voltage (and phase) is measured with LIA-1, and the reference voltage and phase from RC2 is measured with LIA-2. RC3 is used for inductive compensation. The magnitude of the compensation signal is made variable using a variable resistor.

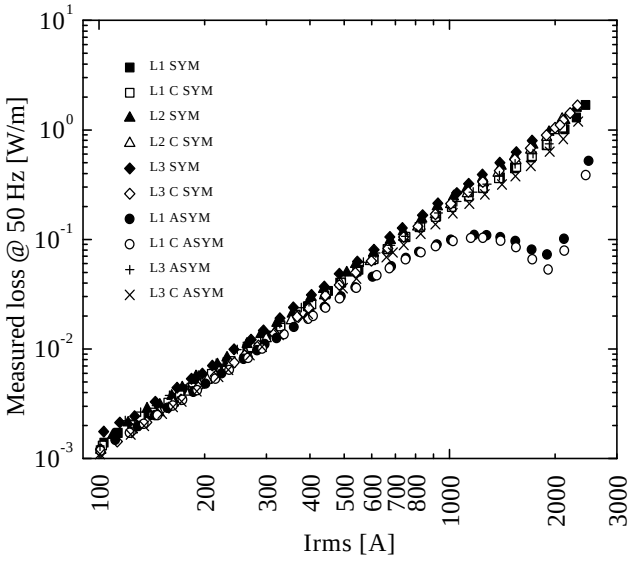

Figure 16. Measured AC-loss (incl. joint resistance) for all configurations under test. ("C" stands for inductive compensation and "SYM/ASYM" stands for symmetric or asymmetric return lead placement, respectively).

The measurements were performed by simultaneously measuring the voltage and the phase angle from the voltage leads (LIA-1) and from RC2 (LIA-2) cf. figure 14. The correct phase for the loss measurement was found by correcting the measured phase of the cable-voltage (from LIA-1) with the phase error of RC1, which was measured with the second lock-in amplifier (LIA-2). Subsequently the data were corrected for the difference in internal phase error of the two lock-in amplifiers.

The difference in internal phase error was found by connecting both lock-in

amplifiers (LIA-1 and LIA-2) to RC2. The result of this procedure was a significant improvement of the phase accuracy - especially at low currents, where it is particularly important to eliminate errors since losses are small and phase angles are close to 90 degrees. The loss was calculated by multiplying the derived in-phase rms-voltage with the measured rms-current.

	R	*m*
L1 SYM	1.24 μΩ	3.30
L1 C SYM	1.18 μΩ	3.26
L2 SYM	1.33 μΩ	3.27
L2 C SYM	1.08 μΩ	3.33
L3 SYM	1.36 μΩ	3.20
L3 C SYM	1.03 μΩ	3.30
L1 ASYM	÷	÷
L1 C ASYM	÷	÷
L3 ASYM	To much scatter in data	
L3 C ASYM	1.02 μΩ	3.34

Table 2. Fitted joint resistances for 8 layer cable.

As the inductive component of the measured voltage typically is much larger (100 to 500 times) than the resistive component the use of an inductive compensation circuit was evaluated. All measurements were performed both *with* and *without* the use of inductive compensation. The compensation circuit was adjusted so that the phase angle was brought down to about 86° at low currents. If the resistive voltage component, i.e. the in-phase voltage, equals 0.1 mV at a phase angle of 89.9° (typical values) then the inductive compensation voltage required for bringing down the phase to 86° is 55.8 mV. The error in resistive voltage introduced by an inductive compensation with a phase error of $\pm 0.01°$ is in this case $55.8\ \text{mV} \times \cos(90 \pm 0.01) = \pm 0.0097$ mV, equivalent to ±10 % of the resistive component. However, as it will appear later in this paper the *final* result of the AC-loss measurements presented is actually *insensitive* to small linear errors in the compensation circuit. The reason for this is that we extract the non-linear losses of the superconductor from the measured data and disregard linear resistive losses, primarily stemming from the copper joints.

Our inductive compensation circuit is made of RC3 connected to a resistive voltage divider cf. figure 14. This circuit is coupled in series with the voltage signal from the cable conductor. The phase error produced by the presence of the variable resistor (voltage divider) depends strongly on the value of the resistor. Its value should preferably be much smaller than the input impedance of the lock-in amplifier (10 MΩ), but also much higher than that of the Rogowski coil, RC3. A voltage divider of 5 kΩ was used for the investigations in this paper.

The LIA manufacturer specifies a relative phase precision of 0.01°, but only an absolute accuracy of <1°. A phase error of ± 0.02° (as we use two LIAs) in the uncompensated signal at 89.9° will correspond to an error of ± 20 %. Compensated data with phase angles at 86° (or below) are not sensitive towards systematic phase errors in the system, e.g. an error of ± 0.02° corresponds to less than ± 1 % at 86°. In figure 16 the total loss vs. current is shown for all the loops and lead configurations tested. It is noticed that the measurements carried out using voltage leads L1 with asymmetric current return lead position differ significantly from the rest of the data. The position of the return leads is clearly affecting the voltage in measurement loop L1, while it only has little effect on the rest of the data. Why the data acquired with the loop L1 and the asymmetric return lead placement (ASYM) with and without compensation differ significantly from the data

acquired using the other loops and configurations is not clear. In single tape conductors an effect of the lead extension on the loss has been observed as a result of the demagnetisation effect produced by the shape of the conductor [19]. If the same reason holds here, then some asymmetry of the current flow might be responsible for the deviation of the results of the L1/L1-C ASYM data from the data obtained with all other voltage- and current return lead configurations. The speculative cause of this could possibly be an asymmetric current saturation in one of the layers of the cable caused by the magnetic field of the asymmetric return lead position. Possibly the L1 loop is more sensitive to the resulting local inhomogeneity of the magnetic field than the loops further away. In the symmetric return lead position there is a significantly reduced magnetic field at the location of the conductor, thus possibly reducing this effect.

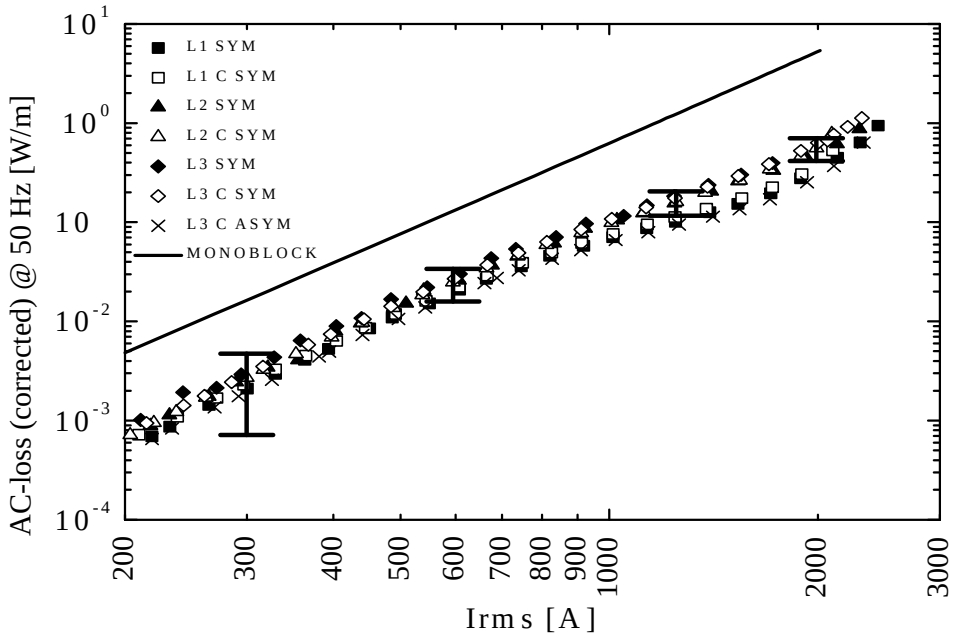

Figure 17. AC-loss corrected for the joint resistance as a function of current. For loop L2-C SYM error bars are shown corresponding to an error in the joint resistance of ± 0.2 μΩ. "C" denotes inductive compensation and "SYM/ASYM" stands for symmetric or asymmetric return lead placement.

The joint resistance is frequency dependent due to the skin effect. Hence, the DC value (0.7 μΩ) can not be used for correction of the loss measurements. The joint resistance, R_j, is found by fitting the measured loss, P, at low currents with the expression

(53) $$P = A \cdot I^m + R_j \cdot I^2$$

where the first term on the right hand side represents the AC-loss in the cable conductor (A and m are constants) and the second term represents the resistive loss in the joint. I is the rms current. It is well acknowledged that eddy current losses are 10-100 times lower than the hysteresis loss [38]. This leaves only the resistive losses of the joints. As the fitting

only is possible when m and R_j actually *are* constant the data is checked for this relationship. This is done by plotting the measured loss divided by the current squared vs. the current (P/I^2 vs. I). The constant m is no longer constant when the data stops being linear in a double logarithmic co-ordinate system at high currents. In table 2 the deduced joint resistances, R_j, are shown together with the found constants m. In all cases m is found to be close to 3.3. In the case of loop L1 ASYM and L1-C ASYM the joint resistances are not calculated as the data appear to be affected by the current and voltage lead positions as discussed earlier in this paper. The joint resistance is also not found for the L3 ASYM data, as these data contain so much scatter at low currents that a meaningful fit could not be made. From the numbers presented in table II it appears that the joint resistances determined from the data obtained with the uncompensated loops and symmetric return lead placement are consistent with a mean value of about 1.3 μΩ. The relative difference between the highest and the lowest joint resistance is found to be only about 10 %. For the data obtained with the compensated loops the consistency is somewhat worse. Here the relative difference is about 20 %. The highest value (which is close to the values derived without inductive compensation) is found for the smallest loop size, L1, and the lowest value is found for the largest loop size, L3. It looks as if more inductive compensation causes lower apparent joint resistance (more inductive compensation is needed for bigger loops as the inductive pick-up increases with the loop area). The reason for this, we believe, is that the compensation circuit not only produces an inductive voltage of sign opposite to the voltage over the cable conductor, but also produces a, however small, *resistive* voltage of sign opposite to the resistive voltage over the cable. A voltage *in*-phase with the cable current can be produced by the current in the compensation circuit which causes self-induction in the coil. The complex current in the compensation circuit is $-d\varphi_{ext}/dt \times (R + j\omega L)^{-1}$, where φ_{ext} is the flux in the coil produced by the current in the cable, L is the self-inductance of the coil, R is the total resistance of the compensation circuit, and ω is the angular frequency. Since $-d\varphi_{ext}/dt = j\omega M I_{cab}$, the voltage over the voltage divider becomes proportional to $(\omega L + jR)$. Here M is the mutual inductance between the cable conductor and RC3; I_{cab} is the amplitude of the current in the cable. Thus if R is not much larger than ωL, a significant in-phase component will be present. For the phase angle to be less than 0.02° from 90° the corresponding R/ωL ratio should be higher than $\tan(89.98°) \approx 3000$. The estimated inductance of RC3 is $L = 4 \pm 2$ mH. Thus the R/ωL ratio is about $5\ k\Omega / 50\ Hz \times 2\pi \times 4 \pm 2\ mH \approx 2600\text{-}8000$. The found reduction of approximately 0.2 μΩ in the apparent joint resistance for the L3 C loop data corresponds to a phase shift in the compensation circuit of 0.02°.

However, we are not directly interested in the joint resistance itself, but actually want to subtract losses scaling with I^2 from the data. The result can be seen in figure 17 where AC-loss data are presented for each data set after correction for the loss with the found (apparent) joint resistances. There is virtually no difference between data obtained for the same loop with or without inductive compensation. For comparison the AC-loss calculated using the monoblock model is also shown:

Even though the AC-loss data obtained with L2 SYM, L2-C SYM, L3 SYM and L3-C SYM appear to be consistent, it can not be excluded that elevating the voltage leads further above the conductor surface will give slightly higher AC-loss data - even in case of

symmetric return lead placement (which is only two-fold symmetric). The conductor loss at 2 kA is found to be 0.6 ± 0.15 W/m.

3.6.3 Resonance method

The circuit diagram for the parallel resonance circuit is shown in figure 18. It consists of the cable, represented by its inductance L_1 and its current dependent resistance (due to the ac loss) R_{ac}. The resistance of current leads and contacts is represented by R, in series with an optional inductor L_2, having a resistance R_2. The resonance circuit is completed by the capacitance C_1, which typically will consist of many capacitors in parallel. The circuit is charged up to the critical current by a dc source over the switch S_1 in the closed state (S_2 closed). The dc voltage on the cable could actually be measured at the cable at this point to determine its dc critical current. When the switch S_1 is opened, the current has no way to

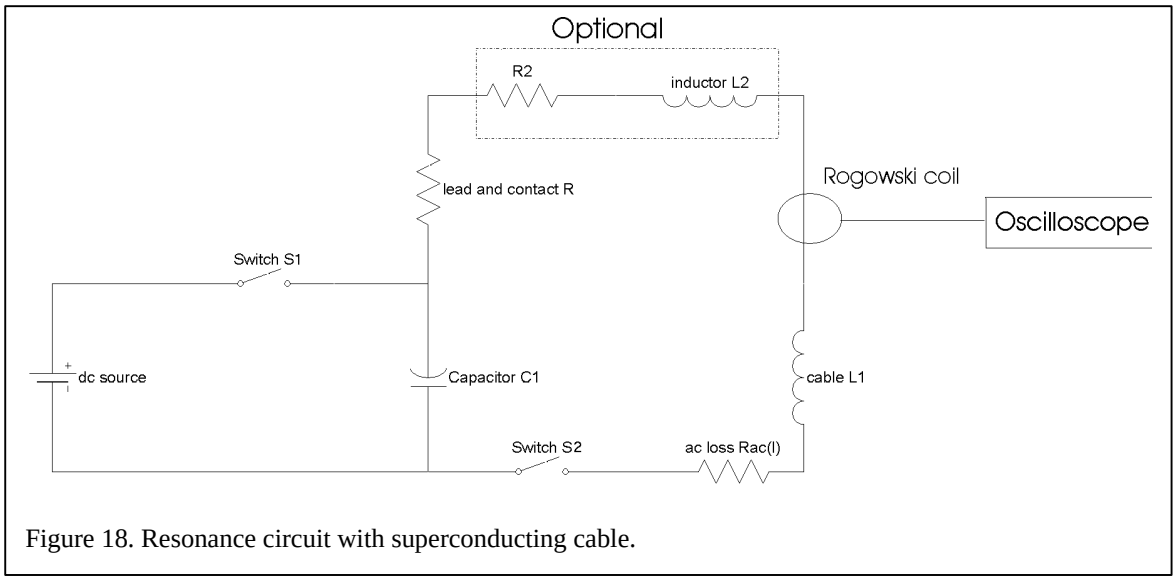

Figure 18. Resonance circuit with superconducting cable.

go as to charge the capacitor C_1, and oscillations will start. The magnitude of the ac current is then measured by the Rogowski coil, the output of which is measured as a function of time using an oscilloscope. Alternatively the voltage on the capacitor can be measured. In this mode of operation the energy in the circuit $1/2\ L_{tot}\ I_o^2$ is supplied by a dc source, where L_{tot} is the total circuit inductance and I_o the initial current.
In a second mode of operation the switch S_2 is initially open, S_1 closed. The dc source now charges the capacitor C_1 up to a certain pre-set voltage, which determines the energy $1/2\ C_1\ V_o^2$ in the system. Then S_1 is opened, and the oscillations are started by closing the switch S_2. In this second mode voltage and current will oscillate as [39]

(54) $I = I_0\, e^{-\delta t} \sin(\omega_r t)$
(55) $V = V_0\, e^{-\delta t} \cos(\omega_r t)$

where $\delta = R_{tot}/2L_{tot} = (R+R_{ac}(I))/2L_{tot}$, and $\omega_r^2 = (2\pi f_r)^2 = \omega_0^2 - \delta^2$, f_r being the resonance frequency. The undamped frequency is given by $\omega_0 = (L_{tot}C_1)^{-1/2}$. R_{tot} and L_{tot} are the total resistance and inductance in the circuit, respectively. A periodic oscillation is only

expected if $\delta<\omega_0$. The damping of the current is caused by the energy loss in the system - mainly in the Ohmic resistance and the ac loss in the superconductor. In the first mode of operation the sin in equation 1 is replaced by a cos, and vice versa in equation 2. It should be noted that the superconductor is a non linear element, so that the sinusoidal shape of the oscillations no longer holds for vanishingly small resistive losses in comparison with the losses in the superconductor.

When cos ($\omega_r t$)=1 all of the energy is stored in the capacitor. Then the energy E(t) in the system as function of time can be expressed as function of the peak voltage V_p

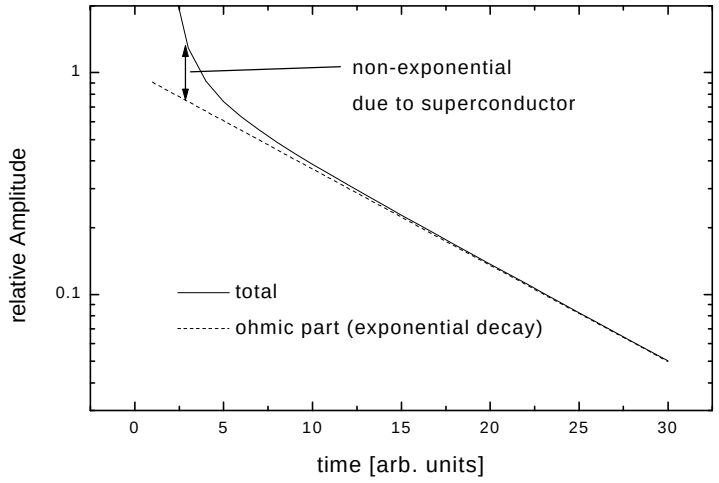

Figure 19. Principle of operation. The amplitude A of the oscillation decays with time due to losses in the superconductor and joint resistances.

(56) $E(t) = 1/2\ C\ V_p^2$

Then the power loss P_{ac} =dE/dt, leading to

(57) $P_{ac} = C\ V_p\ dV_p/dt$

This is also true for a non-linear oscillation. The expected amplitude of the envelope (the maxima of the sine curve) is plotted schematically as a function of time in figure 19. As the resistance of the superconductor (its ac loss) depends strongly on the current (typically $R_{ac} \propto I^2$) a non-linear curve is expected in a log-linear plot. However, once the current I_0 has decayed to a sufficiently small value compared to the critical current of the superconductor one would expect its power loss to be negligible compared to the loss in the Ohmic resistors in the circuit. Thus for longer times the decay curve should become a pure exponential decay, allowing the determination of the size of the Ohmic resistance R in the circuit. Since R is independent of current it is possible to extrapolate the loss due to it down to

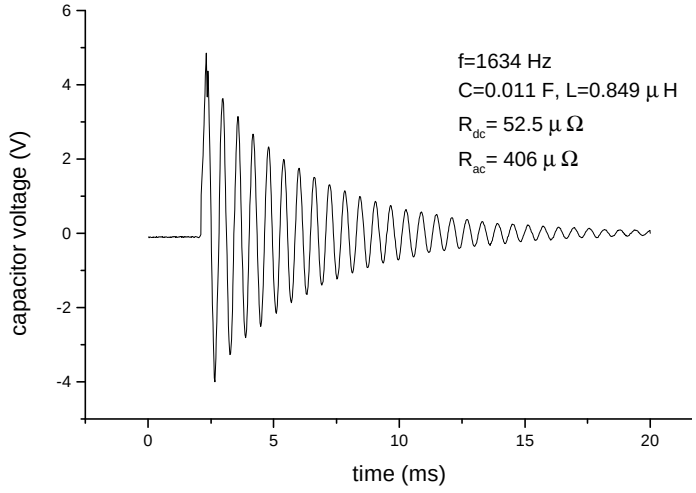

Figure 20. Experiemntal decay of Voltage in test curcuit.

smaller times. Thus the voltage due to the superconductor is simply the difference between the two curves. The RESCUE method has thus an intrinsic calibration.

For a single layer laboratory scale cable conductor the self inductance is of the order of 1μH/m. The capacitance desirable to obtain a resonance frequency of 50Hz (the frequency of interest for applications) is about 1F, a very large value. To achieve a capacitor bank with 1F many thousands of capacitors used for electric motors would have to be put in parallel (this is a true ac application, and thus electrolytic capacitors cannot be used in a straight forward fashion). This is possible and would also provide the necessary current carrying capability, but costly and not too practicable. If the requirement for the resonance frequency is eased to 500 Hz then a capacitor of 10mF is sufficient. An easier way to lower the resonance frequency into the vicinity of 50 Hz is to add an extra inductor. For example 9 (22) turns of copper wire or braid with a diameter of 0.6m have an inductance of 40(400) μH [40], bringing back the resonance frequency to around 100Hz. With an extra inductor L_2 care has to be taken to minimise its Ohmic resistance, possibly by also placing it into liquid nitrogen. It should be noted that the frequency dependence of the hysteretic losses in the superconductor is linear up to frequencies around 1kHz [41]. Thus there is no absolute need to push down the resonance frequency to 50Hz. A drawback of adding extra inductance is the additional resistance added in the circuit. A variant of the method described above using a specially wound superconducting coil of high inductance to measure the ac loss of specimens inserted into it has been described in the literature [42].
In the future quasi-continuous operation of the proposed method could be achieved by developing a small electronic circuit that keeps the oscillation amplitude constant. This could be done by for example by measuring the voltage on the capacitors, and adding energy using well dosed short pulses (of known energy) at the voltage maximum in order to achieve the same amplitude as the previous oscillation. These compensation techniques are well-known and often used in electronics. The ac loss is then given by the energy input into the circuit for a given amplitude. A capacitor bank was constructed containing 100 capacitors in parallel with the nominal capacitance of 100 μF each. The measured total capacitance (using an RC circuit) after construction turned out to be 11.0 mF. A superconducting cable model constructed from Bi2223 tapes was used for experiments. It is 1.1m long, and consists of a single layer of 32 tapes helically wound onto a fibreglass former. Its dc critical current (77K, self field) on first cooldown was 420 A (1μV/cm criterion), with a rather broad transition. Some damage

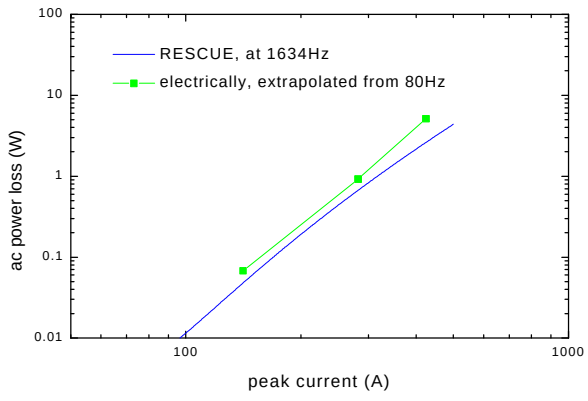

Figure 21. Ac loss determined by RESCUE and comparison with electrical method.

occurred during subsequent cooldowns, degrading the critical current to about 320A. However, the ac loss measured by the 4-probe method does not show the typically expected sharp increase of the ac loss at the degraded critical current as it is seen for example in single tapes.

For the tests reported here the capacitor bank was placed directly above an open bucket type cryostat, keeping the connections short. An additional inductor was not used, so that the circuit inductance was rather low - and thus the resonance frequency rather high. A dc current supply was used to charge the circuit. The voltage on the capacitor bank as a function of time was measured using a LeCroy digital oscilloscope. It is shown in figure 20 for an initial charging current of 500A. A dc circuit resistance of $52.5\mu\Omega$ can be calculated from the dc voltage before the oscillations start. The resonance frequency is 1634Hz, leading to a circuit inductance of L_{tot}=0.849 μH. The Ohmic circuit resistance is calculated to be R_{tot} = 406 μΩ at the resonance frequency. This value includes all contacts, leads and the internal resistance of the capacitor bank. The non-linear decay of the current schematically shown in figure 19 could be observed experimentally, but only for the first few oscillations and much smaller in magnitude than indicated in the figure. In order to obtain a more accurate notion on the superconductor contribution the whole decay curve was fitted to equation 55. For this purpose the data prior to the first peak in voltage was cut off, and the rest fitted. The fit and the data cannot be distinguished in the figure. The result of the fit is a time dependent resistance in form of a 3rd. order polynomial. This time dependent resistance can be remapped into a current dependent resistance using the measured time dependence of the current. The resulting loss in the superconductor can be obtained in two ways: either the deduced apparent resistance is multiplied by the square of the rms current value obtained from figure 20, or equation 55 is used. Both methods agree, and give the curve shown in figure 21. Using the four probe method a loss of 0.3W was measured at a current of 300A (rms) and 80Hz, corresponding to 6W at 1600Hz (if the loss

Acknowledgements

References

[1] C.Rasmussen and S.K.Olsen, Inst. Phys. Conf. Series 158 (Applied Supercond. 2), 1441 (1997)
[2] S.Mukoyama et al, IEEE Trans. Appl. Supercond. 7, 1096 (1997)
[3] K.Sato et al., IEEE Trans. Appl. Supercond. 7, 345 (1997)
[4] M.Leghissa et al., Inst. Phys. Conf. Series 158 (Applied Supercond. 2), 1191 (1997)
[5] A.Bolza et al., IEEE Trans. Appl. Supercond. 7, 339 (1997)
[6] N.Futaki et al, presented at 10th ISS, Gifu, Japan (1997)
[7] J.W.Lue et al., IEEE Trans. Appl. Supercond. 7, (1997)
[8] M.Tinkham, *Introduction to Superconductivity*, McGrawHill (1975).
[9] D.R.Clarke and M.Däumling, "Oxide Superconductors" , chapter 15 in Vol.11 of Materials Science and Technology", edited by R.W.Cahn, P.Haasen und E.J.Kramer, VCH Verlagsgesellschaft (Weinheim, 1994).
[10] C.P.Bean, Rev. Mod. Phys. 36, 31 (1964)
[11] A.Campbell and J.Evetts, Adv. Phys. 21, 199 (1972).
[12] M.Wilson, *Superconducting Magnets*, Clarendon Press Oxford (1983)
[13] W.J.Carr, Jr., IEEE Trans. Magn. MAG-15, 240 (1979)
[14] J.J.Rabbers et al., IEEE Trans. Appl. Superc.9, 1185 (1985).
[15] E.H.Brandt, M.Indenbom, Phys.Rev.B48, 12893 (1993)
[16] W.T.Norris, J.Phys. D3, 489 (1970).
[17] M.Däumling, Physica C 310, 12 (1998).
[18] G.Vellego and P.Metra, Sup.Sci. Techn. 8, 476 (1995).
[19] S.Fleshler et al, Appl. Phys. Lett. 67, 3189 (1995).
[20] St. Clerc, Ph.D. thesis, PSI Villigen (CH).
[21] K.H.Müller and K.E.Leslie, Trans. Appl. Superc. 7, 306 (1997).
[22] C.Schmidt, Cryogenics 34, 3 (1994)
[23] N.Magnussen, S.Hörnfeld, Rev. Sci. Instr. 69, 3320 (1998)
[24] J.A.Eikelboom, Cryogenics 31, 363 (1991)
[25] S.Krüger Olsen et al., IEEE Trans. Appl. Supercond.9, 416 (1999).
[26] M.Däumling, Cryogenics 39, 759 (1999).
[27] H.Noji, Supercond. Sci. Techn.10, 552 (1997).
[28] S.Takács, Supercond. Sci. Techn. 10, 733 (1997), and references therein.
[29] L.Dresner, Appl. Superc. 4, 167 (1996)
[30] W.Lue et al., IEEE Trans. Appl. Supercond. 9, 416 (1999)
[31] S Krüger Olsen et al., Supercond. Sci. Techn.12, 360 (1999).
[32] C.Træholt et al, IEEE Trans. Appl. Superc. 9, 766 (1999).
[33] J.Anders, '*Rating of electric power cables*', IEEE Press New York, 1997.
[34] E.Cereda et al, Physica C 310, 231 (1998)
[35] D.E.Daney et al., Adv. Cryog. Eng. Materials 44, (1998)
[36] J.Rieger et al, Physica C 310, 225 (1998)
[37] M.Däumling et al., Super. Sci. Techn. 11, 1306 (1998)
[38] Y. Fukumoto et al., J. Appl. Phys. 78, 4584 (1995).
[39] R.Becker, *'Electromagnetic fields and interactions'*, Dover, New York, 1982.

[40] F.W.Grover, '*Inductance calculations'*, D.van Nostrand Company, New York 1946.
[41] H.Eckelmann et al. Physica C 295, 198 (1998).
[42] T.Ishigohka et al., Cryogenics 34, 575 (1994)